Multi-Cell Admission Control for WCDMA Networks

GUSTAVO AZZOLIN DE CARVALHO PIRES

Multi-Cell Admission Control for WCDMA Networks

GUSTAVO AZZOLIN DE CARVALHO PIRES

Master's Degree Project

29th, May 2006

School of Information and Communication Technology
Department of Communication Systems

Abstract

It has long been recognized that in multi-cell WCDMA networks the admission of a new session into the system can have undesirable impact on the neighboring cells. Although admission control algorithms that take into account such multi-cell impact have been studied in the past, little attention has been paid to multi-cell admission and rate control algorithms when traffic is elastic. In this thesis, we propose a model for multi-cell multi-service WCDMA networks to study the impact of multi-cell admission and rate control algorithms on key performance measures such as the class-wise blocking and outage probabilities, block error rates, and the noise rise violation probabilities. By means of simulation we compare the performance of load based multi-cell algorithms with that of a single cell algorithm. We find that with multi-cell based algorithms the system capacity and performance (in terms of the above mentioned measures) are (in some cases significantly) better in homogeneous load scenarios as well as in the heterogeneous 'hotspot' and 'hotaround' scenarios.

Keywords: WCDMA, Elastic Traffic, Admission Control, Rate Control, Blocking Probability, Outage Probability

Sammanfattning

Det har länge varit känt att i multi-cellulära WCDMA nät så kan insläppandet av en ny användare i systemet ha en icke önskvärd effekt på intilliggande celler. Fastän insläppskontrollalgoritmer (AC) som tar hänsyn till sådana multi-cellulära effekter har studerats tidigare, så har endast begränsad uppmärksamhet ägnats åt multi-cellulär insläpps- och bittaktskontrollalgoritmer när trafiken är elastisk. I detta arbete föreslår vi en modell för WCDMA-nät med multipla celler och multipla tjänster och som är applicerbar för studier av av hur multi-cellulär insläpps- och bittaktskontroll inverkar på viktiga prestandamått som klassvisa spärr- och utslagningssannolikheter, blockfelssannolikheter, och sannolikheten för överträdande av tillåten interferensnivå. Med simuleringar jämför vi prestanda för lastbaserade multi-cellalgoritmer med prestanda för singel-cellalgoritmer. Vi har funnit att med multi-cellalgoritmer så är systemskapacitetet och prestanda (i termer av tidigare nämnda mått) i några fall betydligt bättre i homogena lastscenarier, samt i heterogena lastscenarier av typerna 'hotspot' och 'hotround'.

Keywords: WCDMA, Elastisk Trafik, Insläppskontroll, Bittaktskontroll, Spärrsannolikhet, Utslagningssannolikhet

This page intentionally contains only this sentence.

Acknowledgements

This work has been performed as a degree project at Ericsson Research, Stockholm during the period September 2005 - April 2006. I would like to express my sincere thanks to:

Prof. Gerald Q. Maguire Jr., my supervisor at KTH, for his inspiring guidance, rapid replies, and valuable suggestions;

Gabor Fodor, my supervisor at Ericsson AB, for providing me with a deep and complete understanding of this project, giving me autonomy to drive my project, and his patience during the project;

Ericsson AB, especially for giving me the opportunity to perform my thesis Project;

A special thank to Birgitta Olin, Nicolas Debenardi, and Jean-Christophe Laneri, who helped me with the simulations;

I also want to express my gratitude to my friends and ex-girlfriend, for their support.

This page intentionally contains only this sentence.

Contents

List of Tables

This page intentionally contains only this sentence.

List of Figures

List of Abbreviations

3G	3rd Generation of Cellular Networks
3GPP	3rd Generation Partnership Project
AC	Admission Control
AICH	Access Indication Channel
BCH	Broadcast Channel
CDMA	Code Division Multiple Access
CN	Core Network
DCCH	Dedicated Control Channel
DPCCH	Dedicated Physical Control Channel
DPDCH	Dedicated Physical Data Channel
DSAC	Dynamic Soft Admission Control
DS-CDMA	Direct Sequence Code Division Multiple Access
DTCH	Dedicated Transport Channel
E-DCH	Enhanced Dedicated Channel
EDGE	Enhanced Data GSM Environment
FDD	Frequence Division Duples
FDMA	Frequence Division Multiple Access
GPRS	General Packet Radio Service
GSM	Global System for Mobile Communications
HARQ	Hybrid Automatic Repeat Request
HSDPA	High Speed Downlink Packet Access
HSUPA	High Speed Uplink Packet Access
LC	Load Control
MC	Multi-cell

MCF	Multi-cell Fair
NAS	Non Access Stratum
NR	Noise Rise
PS	Packet Scheduling
PRACH	Physical Random Access Channel
QoS	Quality of Service
RAB	Radio Access Bearer
RAN	Radio Access Networks
RNC	Radio Network Controllers
RPCAC	Received Power Admission Control
RRM	Radio Resources Management
SA	Scheduling Algorithms
SC	Single-cell
SFN	System Frame Number
SINR	Signal-to-Interference to Noise Ratio
SIR	Signal-to-Interference Ratio
SSAC	Static Soft Admission Control
TDD	Time Division Duplex
TDMA	Time Division Multiple Access
TPCAC	Transmitted Power Call Admission Control
TTI	Transmission Time Interval
UE	User Equipment
UMTS	Universal Mobile Telecommunication Services
UTRAN	UMTS Terrestrial Radio Access Network
WCDMA	Wideband Code Division Multiple Access

Chapter 1

Introduction

With the recent introduction of 3G services, new demands for quality of service have been created. The possibility of transmitting all kinds of media through cellular telephone networks has increased substantially during the last few years. The actual 3G specification has gone through several releases, each revision has introduced new requirements, for instance, handling multiple classes of users, simultaneously in a fair scheduling and sharing schema.

Unlike time-division multiple access (TDMA) networks, where Admission Control is simply based on allocation to one or more available physical channels, code-division multiple access (CDMA) networks are strongly connected to the physical layer performance since the multi-access interference in the system depends directly on the current number of users. Therefore admission control is a limiting factor to ensure that the system meets the Quality of Service (QoS) guarantees.

A CDMA system, just as any other communication network, has limited resources; hence, there are a limited number of users (with fixed demands) or packets (in the case of variable demands) that should be allowed into a network at any given time. Such discussions are naturally related to the economics of networks, as some choose to operate close to a full capacity. In this context, there are some considerations, particularly related to QoS, that require operating at a lower capacity level.

We know that the greater the offered packet traffic load, the greater the delay experienced by packet transmissions, due to the finite amount of resources. In other words, the more packets allowed into a network (once the load is past some limit), the lower the experienced QoS. Thus, in order to maintain specific QoS commitments there is a need to limit the number of calls and their traffic. On the other hand, limiting the number of calls not only affects potential revenue, but this can also eventually create a bad impression from the customer's perspective, if the operator is consistently unable to offer a certain service. In this sense, operators have an interest not only in end-to-end delay, but also other QoS measures, such as data throughput. Additionally, the operators are also interested in reducing the call-blocking probability. Good practice in the telecom industry is to have a blocking probability of less than 5 percent and preferably only 1 to 2 percent interval.

QoS provisioning is related to the operator's ability to provide different types of services, which should fit different traffic classes. When implementing QoS provisioning, some set of desired QoS parameters is negotiated between the customer and the operator.

In this context Admission Control has emerged as one of the main means of QoS provisioning. The basic principle of Admission Control is to admit a new user into the system only when the user's QoS requirements can be sufficiently satisfied, as well as satisfying all existing users' requirements. Admission Control algorithms should be able to avoid false accepted calls, meaning that existing QoS provisioning could be affected with such an admission, and also false rejected calls due to an overly conservative admission algorithm approach.

Moreover, in wide-band CDMA networks, based on shared interference, Admission Control should be considered on an entire-system-basis, i.e. in a multi-cellular environment, as well as considering the dependence on other QoS provisioning related algorithms such as power and rate control. As a new contribution, this thesis project involved the designs and evaluation of Single and Multi-Cell Admission Control algorithms associated with slowdown, i.e. rate controlled mechanisms. An existing WCDMA

simulator [25] was utilized as the simulation platform, and results, referred to capacity and QoS, indicate multi-cell radio resource mechanisms as significant means to ensure high resource efficiency in addition to user satisfaction.

The thesis begins with a general overview of the Universal Mobile Telecommunication Services (UMTS), followed by a brief introduction to Radio Resources Management. Chapter 4 examines Admission Control Algorithms with a focus on the Uplink, which is interference limited.

Chapter 2

Universal Mobile Telecommunication Services(UMTS)

The standard for third generation mobile communication system in Europe is referred to as *Universal Mobile Telecommunication Services* (UMTS). This standard is regulated by the *3rd Generation Partnership Project* (3GPP), an important body of the *European Telecommunications Standards Institute* (ETSI). The radio interface used in UMTS that we considered is *Wideband Code Division Multiple Access* (WCDMA). The following sections will a give short introduction to WCDMA for UMTS, present some key concepts in past and future releases of UMTS, e.g. *High Speed Uplink Packet Access* (HSUPA), and finally introduce some theory related to the Uplink in WCDMA. More details about UMTS can be found in [12] and [1], while basic principles of wireless communications are in [10].

2.1 UMTS Network Architecture

The UMTS network basically consists of a *Core Network* (CN), *Radio Network Controllers* (RNCs), *Base Stations* (Node Bs), and *User Equipment* (UE). Figure 2.1 gives a schematic picture of a UMTS network, showing some of its fundamental elements.
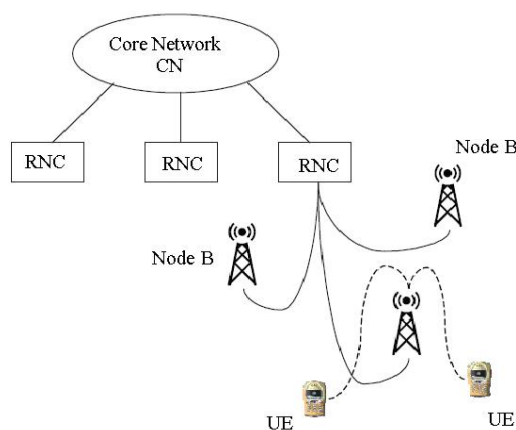
Figure 2.1: Overal UMTS Architecture

The UE can be a mobile phone or a computer interface. The RNC and Node B together constitute the *Radio Access Network* (RAN), providing the connection between the UE and the core network. Each

RNC controls a number of Node Bs. The radio signal is transmitted and received by a Node B. Each Node B supports one or more cells covering a geographical area. If the site is a three-sector type, then the Node B provides three cells. Each UE within a cell is connected to at least one Node B. As the cells normally intersect near the cell borders, UEs positioned in this overlap area can be connected to more than one Node B.

Here we have included in the core network of an UMTS network a number of functions:

- Call Control - The CN handles the setup, maintenance, and release of voice, packet, Short Message Service (SMS), and Multimedia calls.

- Mobility Management

- Charging

- Subscriber data management

- Service Control

- Security

The Core Network also controls the interfaces to access networks for *GSM Base Station System* (BSS), WCDMA RAN, and external networks.

New releases of the UMTS standard are transferring some key functions from the RNC to the Node B in order allow more efficient link adaptation. For example, in Release 5 *High-Speed Downlink Packet Access* (HSDPA) is introduced, to support this key media access and control (MAC) functions now reside in the Node B (i.e. fast scheduling and link layer feedback).

2.2   Introduction to WCDMA

In the previous generations of mobile communication systems, users were separated and organized by transmitting in different time slots, for the *Time Division Multiple Access* (TDMA) and/or using different frequencies, for the *Frequency Division Multiple Access* (FDMA) technique. In the *Wideband Code Division Multiple Access* (WCDMA) users are organized based upon their use of spreading codes. This makes it possible for several users to transmit at the same time on the same frequency.

WCDMA uses *Direct Sequence CDMA* (DS-CDMA). In this technique, the original signal is spread by multiplying the signal with a specific spreading code, consisting of a sequence of 1 and -1 bits, which are also called chips. The spreading codes are chosen from a certain code tree, similar to the one shown in Figure 2.2. Different levels of the code tree correspond to different code lengths. Assuming that a user has been reserved a code, codes in the subtree of that code are longer available. This preserves orthogonality between codes, even for codes with different lengths, thus reducing interference between different codes.

Figure 2.3 illustrates data (signal) spreading and dispreading. In this case, every data symbol is converted to a "spread symbol", by multiplying it by the specific spreading code, in this case with a spreading factor of 8 chips per bit. In this case we say that we have used a spreading factor of 8, i.e. the ratio of the chip rate to the data rate is 8. As we will see in the following sections, the chip rate is also denoted as W and the data rate as R. The multiplication with a spreading code with chip rate greater than the data rate results in an apparently random signal. Multiplying the spread signal with the spreading code, i.e. dispreading, restores the signal to its previous original form, see Figure 2.2.

As we know, signal bandwidth is proportional to the bit rate. Since the original signal, with a specific data rate, is spread by the spreading factor (also called processing gain), the bandwidth will also be increased by the same spreading factor. WCDMA uses a chip rate of 3.84 Mcps, which results in a bandwidth of around 5 MHz. Compared to the earlier CDMA technologies, as the Interim Standard 95 (IS-95) [11], this bandwidth is wider, hence the name Wideband CDMA.

Figure 2.3 illustrates this bandwidth widening through the spreading technique, and how the receiver can easily find and decode the pertinent signal (as it knows the spreading code being used). The
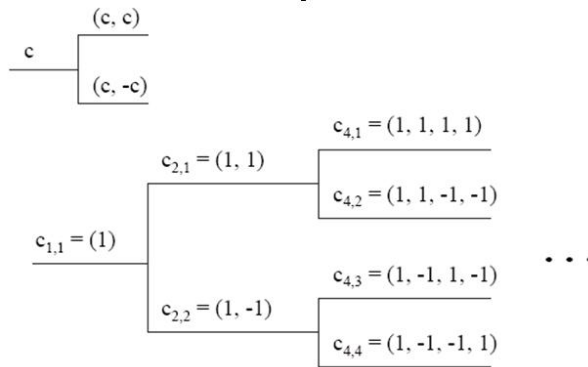
Figure 2.2: Example Channelization Code
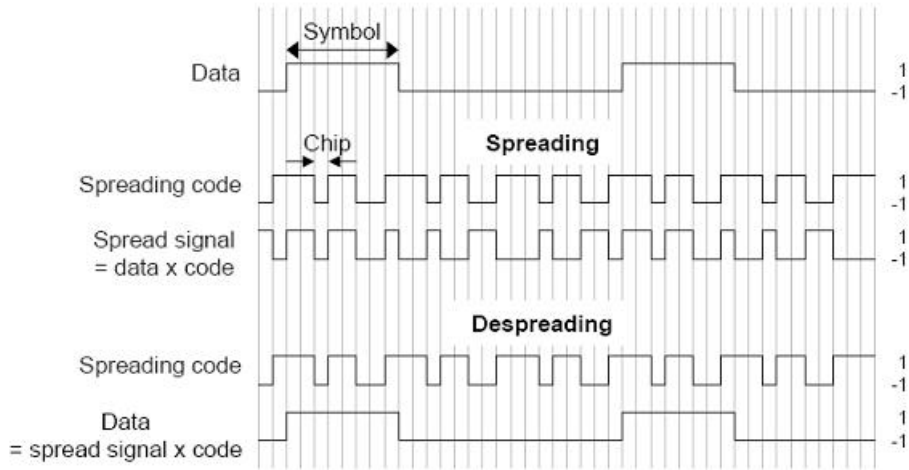
Figure 2.3: Spreading and dispreading in DS-CDMA

same spreading code used to generate the spread signal is used to dispread the transmitted signal, thus recovering the original signal. WCDMA supports two ways of separating the downlink from the uplink channels. This separation is done by Frequency Division Duplex (FDD) or by Time Division Duplex (TDD). The FDD mode is currently the one that vendors implement with WCDMA.
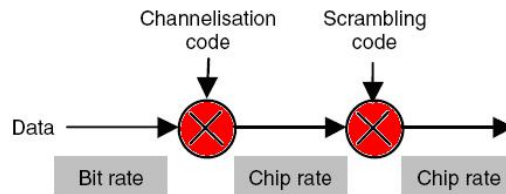
Figure 2.4: Spreading and Scrambling Signal

It is important to understand the difference between scrambling, *spreading*, and channelisation codes.

When one speaks about spreading, signals are first spread using channelisation codes, after which a scrambling code is applied at the same chip-rate as the channelisation code; hence scrambling does **not** alter the signal bandwidth. This is illustrated in Figure 2.4. Channelisation codes are used to separate channels from the same source (i.e. the different downlink channels in one sector or cell or the different uplink dedicated channels sent by one mobile terminal). Scrambling codes are used to separate signals from different sources. In this context a channelisation code represents a signature which uniquely identifies a channel.

2.3   UMTS Statistics

The statistics (taken from [5], october 2005) below are approximate worldwide totals, unless stated otherwise.

- 3G subscribers (UMTS/WCDMA + CDMA2000 EV-DO): 50+ million

- UMTS/WCDMA subscribers: 33+ million

- UMTS/WCDMA subscribers by region: Japan 52.5% ; Europe 43.5% (14+ million); Rest of World 4%

- UMTS/WCDMA devices (units) shipped: > 20 million in 2004

- UMTS/WCDMA network launches: more than 80 operators in over 35 countries

- UMTS/WCDMA device (models) commercially available or announced: more than 180 from over 25 manufacturers

Figure 2.5 illustrates how UMTS/WCDMA has grown worldwide in terms of customers, i.e. subscribers during the year of 2004. Interesting to notice was the limited deployment in the rest of the world, especially America, which reflects a multi-billion dollar battle between different cellular standards.

Figure 2.5: Evolution of number of WCDMA customers -[5]]

The intention with these statistics is to show that WCDMA is still a new technology that has only recently started to have significant uptake. The *Global System for Mobile Communications* (GSM), that had its first specification by 1990, is today the dominant mobile system with 70% of world's market, it continues to still be the focus of research work. In this context, WCDMA, with its almost incontestable position as the next dominant wireless standard for mobile communications, as well as the expectations for new demand and variety of services offered by operators, has been the focus of a large number of current research projects. This thesis addresses radio resource management issues as part of the maturation of WCDMA.

2.4 WCDMA Evolvement

WCDMA is a continuously evolving standard. Figure 2.6 illustrates the basic evolution. In the standardized radio interface for WCDMA release 5, the main concept introduced was *High Speed Downlink Packet Access*(HSDPA). Moreover, the increased demand for data services and the importance of IP based services also require the uplink transmission to support high data rates. Within the 3GPP a concept to improve transmission **from** the cell phone to the base station, called Enhanced Uplink, is being developed. A basic introduction to Enhanced Uplink is presented in the following section. The basics of HSDPA are explained in [13].
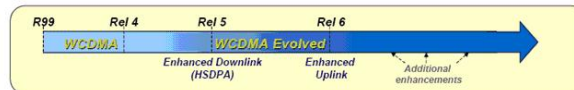
Figure 2.6: WCDMA Evolvement Illustration - [5]

2.5 HSUPA

High-Speed Uplink Packet Access (HSUPA), is a data access protocol for mobile networks with upload speeds up to 5.8 Mbit/s. Together with *High-Speed Downlink Packet Access* (HSDPA), HSUPA (or also *Enhanced Uplink*) is sometimes denotes as 3.5G.

The specifications for HSUPA are still under development and are expected to be included in UMTS Release 6. HSUPA is supposed to include many solutions from HSDPA, but it also has some of its own peculiarities. Details of the Enhanced Uplink concept can be found in [2]. In general, the main goals for Release 6 are to improve *coverage* and *throughput* as well as to reduce the *delay* in the uplink. Among the requirements which have been discussed in the 3GPP [4] is that the enhanced uplink channels should be able to operate together with the current WCDMA releases. For instance, these new channels must not seriously affect current *real time* services, such as speech, which are provided by dedicated channels.

HSUPA introduces a new *Enhanced Dedicated Channel* (E-DCH), which is assigned to only one UE at a time. This channel employs link adaptation methods similar to those defined in HSDPA, namely:

- shorter *Transmission Time Interval* (TTI) enabling faster link adaptation - since the uplink is interference limited, fast link adaptation is necessary. The Node B controls the uplink data rate for every user. Moving this rate control to the Node B reduces delays which leads to faster adaptation and more precise control of uplink interference power. Due to statistical multiplexing of a high rate channel a larger number of bursty high bit rate users can be allowed, thus making better use of the uplink capacity. However, they still must share a single 5.8Mbps channel.

- *Fast Hybrid Automatic Repeat Request* (HARQ) with incremental redundancy making retransmissions more effective: The enhanced uplink supports Node B controlled retransmissions, unlike previous WCDMA releases, where retransmissions commands were issued by the *Radio Network Controller* (RNC). By rapidly requesting retransmission of erroneous data, packet delay is obviously reduced. This proposed new release also employs soft combining, which means that retransmitted blocks are combined with previous erroneous blocks in order to correct the data. Using soft combining reduces the volume of data that must be retransmitted. The lower delays and reduced retransmissions, leads to greater capacity and improved robustness to errors.

As in HSDPA, a *packet scheduler* is utilized to process *request-grants*. A UE requests permission to send data, then the scheduler decides how and when each UE will get to transmit. In the UE's request for transmission there will be information about the state of the transmission buffer and current power constraints. This scheduler is fundamental to HSUPA's *Radio Resources Management* (RRM).

While in UMTS Release'99 the ratio between the power of the *Dedicated Physical Data Channel* (DPDCH) and *Dedicated Physical Control Channel* (DPCCH) was constant, in HSUPA this ratio is controlled by the Node B.

The Node B is also responsible for issuing both *power-up* and *power-down* commands. However, all the Node Bs participating in a handover are only able to issue *power-down* commands. A *power-down* command should take priority over a *power-up* command in order to reduce interference.

2.6   Access Control and QoS Classification

QoS in WCDMA systems is related to the *Radio Access Bearer* (RAB). The RAB is used to transfer user data between the *User Equipment* (UE) and the *Core Network* (CN), i.e. via the *Radio Access Network* (RAN). The RAB contains two channel types. These channel types are the *Dedicated Transport Channel* (DTCH) and the *Dedicated Control Channel* (DCCH). The combination of these two channels allows for traffic classification, for example [16]:

- *Conversational*: speech or voice traffic, with QoS requirements usually set by human perception, e.g. voice calls, SMS, etc.

- *Streaming*: one way user data transfer with a bounded delay requirement.

- *Interactive*: represented by the request-response pattern of data transfer, where a human or machine requests data from a remote entity, e.g. web browsing or data base query.

- *Background*: correct content delivery, but without a specific delay bound, e.g. download of mail.

Each RAB is characterized by certain QoS parameters, including bit rate and delay bound. The following sections will show the reader how the bit rate, power, and interference are connected in CDMA systems. Thus, allowing resources to be consumed by a user will lead to a power increase in the cell.

2.7   Random Access Procedure and Call Admission Control

Random-access transmission in WCDMA is based on a slotted ALOHA approach. Before starting any random-access procedure, the UE listens to the *Broadcast Channel* (BCH) containing available signatures, available slots in the available subchannels, power ramping factor, initial transmission power, persistency value, and maximum allowed preamble transmissions. The UE then randomly picks an available subchannel (*SelSubCh*), an access slot in that sub-channel, and an available spreading code, then it starts to transmit using the respective preamble signature and transmission power. After the Node B receives the preamble, it replies with a positive acknowledge ACK (*Access Indication Channel (AICH) preamble*) or with a negative acknowledgement (NACK), which is expected to follow at τ_{p-a} seconds after the preamble sent in the access slot. The access slot and the AICH access slot are paired and separated by this τ_{p-a} time. Note that the network does not send any reply if no preamble is received due to insufficient transmission power or preamble collisions. If there is no ACK, and the maximum number of retransmissions has not yet been reached, then the UE picks another available access slot and transmits another preamble with power increased by the ramping factor. If the number of retransmissions limit is reached, then the random-access procedure is terminated causing a *random-access procedure failure*. Once an ACK is received, then the UE starts its transmission using the allocated traffic channel.

Access is requested by sending several subsequent preamble transmissions with increasing power at well-defined time-offsets, also as access slots. These preambles are transmitted through a *Physical Random Access Channel*(PRACH). Each PRACH consists of 15 access slots divided in two frames according to Figure 2.7.

These access slots are further divided in 12 sub-channels, each of these defines another sub-set of the total set of uplink access slots that can be used by future preamble transmissions. This mapping can be seen in Figure 2.8 [6]. SFN stands for *System Frame Number*, which provides the UE timing information that is essential to the decoding processes. In other words, for an asynchronous Node B, the UE must
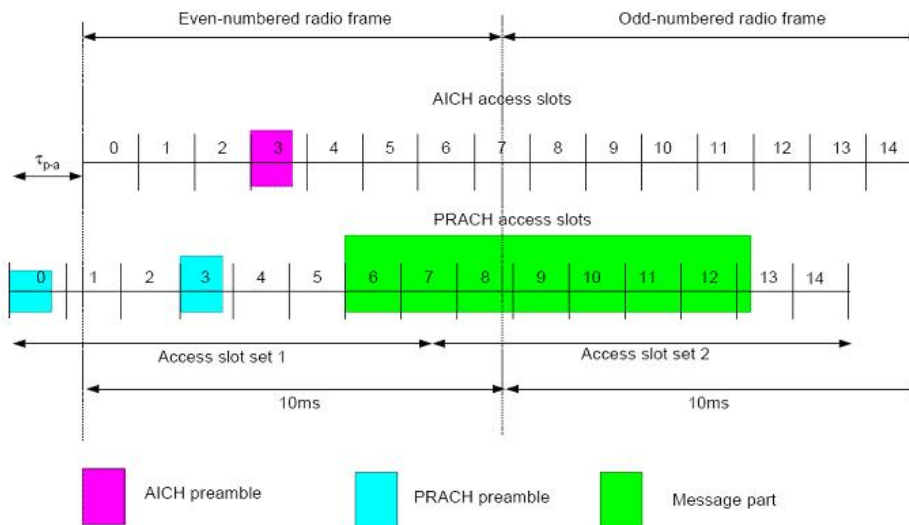
Figure 2.7: PRACH structure

demodulate the BCHs of the neighbouring base stations, read the system frame number and report the relative time difference (SFN-SFN) to the network. This is useful for handover purposes.

SFN Mod 8	Sub Channel Number											
	0	1	2	3	4	5	6	7	8	9	10	11
0	0	1	2	3	4	5	6	7				
1	12	13	14						8	9	10	11
2				0	1	2	3	4	5	6	7	
3	9	10	11	12	13	14						8
4	6	7				0	1	2	3	4	5	
5			8	9	10	11	12	13	14			
6	3	4	5	6	7					0	1	2
7						8	9	10	11	12	13	14

Figure 2.8: Available uplink access slots for different sub-channels

2.8 Summary

This chapter provided the reader with a basic introduction to WCDMA and Admission Control. Spread-spectrum technology is the basis for CDMA networks, and implies the interference control schemes as one of the key aspects. Furthermore, UMTS evolution towards HSUPA has been shortly presented due to its particularities when compared with the WCDMA Uplink from previous Releases. Finally, a brief description about Random Access Procedure, as well as QoS classification have also been introduced considering their inherent relation with Admission Control.

This page intentionally contains only this sentence.

Chapter 3

Radio Resources Management

The *Radio Resource Management* (RRM) functions are responsible for efficiently utilizing the radio interface resources. RRM guarantees Quality of Service and maintains the planned coverage area associated with offering high capacity.

The RRM functions in WCDMA can be divided into:

- Power control

- Handover Control

- Congestion Control:

    - Admission Control

    - Load Control

    - Packet Scheduling
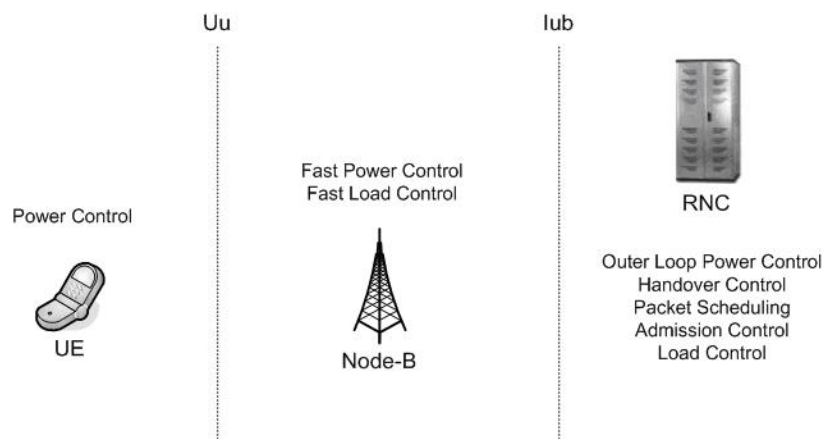
Figure 3.1: Typical locations of RRM algorithms in WCDMA networks

The following sections introduce the above RRM functions, which should help the reader to better understand the relation between Admission Control and other RRM functions.

3.1   Power Control

In WCDMA networks "power" is a finite resource for both the Uplink and Downlink communications. Power control is needed in order to minimize the interference levels, thus providing the required quality of service of the connections. It consists of the following three functions:

3.1.1   Uplink and Downlink Outer Loop Power Control

The Uplink Outer Loop Power Control sets the target quality value for the UL Inner Loop Power Control. It receives input from quality estimates of the transport channel. As in the Uplink, the Downlink Outer Loop Power Control sets the target quality value for the DL inner loop power control. It receives inputs from quality estimates of the transport channel, measured in the UE. The Uplink and Downlink outer loop power control are mainly used for a long-term quality control of the radio channel.

3.1.2   Uplink and Downlink Inner Loop Power Control

The UL Inner Loop Power Control sets the power of the uplink dedicated physical channels. It receives the quality target from UL Outer Loop Power Control and quality estimates of the uplink dedicated physical control channel. As in the Uplink, the Downlink Inner Loop Power Control sets the power of the downlink dedicated physical channels. It receives the quality target from Downlink Outer Loop Power Control and quality estimates of the downlink dedicated physical control channel.

   The Uplink power control commands are sent on the downlink dedicated physical control channel to the UE, while the downlink power control commands are sent on the uplink dedicated physical control channel to the *UMTS Terrestrial Radio Access Network* (UTRAN).

3.1.3   Uplink and Downlink Open Loop Power Control

The Uplink Open Loop Power Control sets the initial power of the UE, i.e. at random access procedure. The function receives UE measurements of interference levels and broadcasted cell/system parameters as input.

   The Downlink Open Loop Power Control sets the initial power of downlink channels. It uses downlink measurement reports from the UE.

3.2   Handover Control and Macro Diversity Control

During handovers, the handover funtion controls the overall handover execution process. It starts the handover process in the entities involved, and receives indications regarding the results. Its main goal is to ensure that the UE is always utilizing the strongest cell, and it also ensures a seamless handover process.

   The handover function may be either controlled by the network, or independently by the UE. Therefore, this function may be located in the RNC, the UE, or both.

   Along with the Handover Control Function comes the Macro Diversity Control Function. Upon request of a Handover process, the macro diversity function controls the duplication/replication of information streams to receive/ transmit the same information through multiple physical channels (possibly in different cells) from/to a single mobile terminal.

   This diversity control function also controls the process of combining information streams generated by a single source (diversity link), but conveyed via several parallel physical channels (diversity sublinks). Macro diversity control should interact with channel coding control in order to reduce the bit error ratio when combining the different information streams. This function controls macro-diversity execution which is located at the two endpoints of the connection element on which macro-diversity is applied (diversity link), that is at the access point (Node-B) and also at the mobile termination.

   The diversity control function is typically located in the UTRAN. However, depending on the physical network architecture, some bit stream combining function within the CN may have to be included.

3.3 Congestion Control

3.3.1 Admission Control

The purpose of the Admission Control Function is to control the admission or rejection of new users, new radio access bearers, or radio links (in handover case). The main objective is to try to avoid overload situations by basing decisions on resource measurements. In this function, decisions can also depend on priority.

The following five approaches for Admission Control will be further explained on the next chapter.

- Hard Admission Control or Hard Capacity, with a fixed number of users

- Soft Admission Control, with different approaches:

    - Received/Transmitted Power Call Admission Control (RPCAC/TPCAC)

    - SIR-based Admission Control

    - Static and dynamic Soft Admission Control

    - Load Estimation based Admission Control

Because of the focus of this thesis work, the above Admission Control approaches are extensively covered in Chapter 4.

3.3.2 Load Control

The Load Control (LC) function normally takes actions that can be grouped into two categories:

- Preventive actions taken to avoid the network from becoming overloaded, thus enabling it to remain stable

- Reactive actions specially taken to bring the network back to a stable operating points when the previous prevention actions did not work.

Classical examples for such actions are: Lower *Signal to Interference Ratio* (SIR) target for the uplink inner loop PC, throttle down packets for data traffic, lower bit rates of adaptive RT users (speech or CS data), or in the extreme case, simply drop single sessions or calls.

3.3.3 Packet Scheduling

Packet Scedulling function aims to ensure that fair and proper resource sharing policies are taken under specific load budget constraints.

In brief, this scheduling controls per-packet access to the radio resources, which includes which type of channel is used (dedicated, common, shared), Quality of Service (QoS) requirements associated with a service, or even the type of resources which the network radio interface is utilizing, i.e. code, frequency, time, or power.

3.4 Load Sharing

Load Sharing considers the overall multi-cell equalized capacity and performance. In other words, this control function aims to distribute sessions among different cells in order to more equally load the system.

3.5 Summary

From this chapter, the reader could understand the relation between Admission Control and the other RRM functions. Since Admission Control is the first RRM function to take place for a call in terms of time, it holds a very important role in order to coordinate with the consecutive RRM functions. Chapter 4 will more deeply examine about Admission Control algorithms and related RRM functions.

This page intentionally contains only this sentence.

Chapter 4

Admission Control Algorithms

Since *Radio Resource Management* (RRM) strategies for Admission Control function are not part of the standard, there are a large number of different proposals available in literature. As mentioned in the previous chapter, the most common ones are:

- Hard Admission Control or Hard Capacity, with a fixed number of users

- Soft Admission Control, with different approaches:
    - Received/Transmitted Power Call Admission Control (RPCAC/TPCAC)
    - Signal to Interference Ratio (SIR)-based Admission Control
    - Static and dynamic Soft Admission Control
    - Load Estimation based Admission Control

In WCDMA networks there are two main factors related to admission control: *Multiple Access Interference* (MAI) and limited transmission power. All active users cause interference to each other, thus affecting the overall quality of all connections, especially in the uplink connections (due to the non-orthogonality of codes in the uplink). The second limiting factor is related to transmission power of the *Base Stations* (BS) on the downlink.

4.1 Admission Control Approaches

4.1.1 Hard capacity or Hard Admission Control

In the hard capacity case, an admission decision is based on a fixed bound on the number of users, or the number of available links. This is the simplest schema to implement, because no calculations regarding the load of the system are made. However, this is not very suitable for CDMA networks where capacity of such systems is naturally "soft", rather than rigid, as in a FDMA or TDMA system. Basically, the problem with this method is that it does not consider the fact that admitting different users produces different load increases in the system. However, this approach was employed in earlier TDMA and FDMA networks.

4.1.2 Received/Transmitted Power Call Admission Control (R/TPCAC)

In the Received Power Admission Control schema for Uplink, new calls are rejected if the total received power at the BS would violate a certain power threshold. This approach reserves some extra power in order to handle handover traffic. It only addresses the uplink admission case. The drawback of this schema is that it does not distinguish between arriving calls with different QoS requirements.

On the other hand, Transmitted Power Call Admission Control is a downlink admission schema, where a new call is rejected when it would cause all the current calls to transmit at maximum power.

Essentially, TPAC implements a setup time where a call is only admitted if all ongoing user constraints are still respected after the convergence time (same as setup time).

4.1.3 "Signal-to-interference-ratio"-based Admission Control

There are several algorithms related to this approach. Since MAI is a limiting factor in CDMA systems, the goal is to keep the Signal to Interference Ratio (SIR) target levels high enough in order to satisfy the QoS needs of the already admitted users. This introduces the term "residual capacity" as the criterion for Admission Control. Residual capacity defines the maximum numbers of additional calls a certain cell can admit such that the QoS requirements of the currently admitted users are still satisfied. This technique can be applied locally, i.e. no consideration is made of the neighbour cells residual capacity, or globally, in which the residual capacity of every cell is related to its impact on adjacent cells.

4.1.4 Static and Dynamic Soft Admission Control

These scheme aim to guarantee, for both ongoing and new calls, that there is an adequate *Signal-to-Interference to Noise Ratio* (SINR), i.e. higher than a pre-defined SINR threshold. This SINR threshold is derived from a set of QoS attributes, which are negotiated between the system and user. These algorithms evaluate the Multiple Access Interference level, enabling the system to prevent the admission of a call that would cause an unacceptable degradation of the overall service quality. Basically *Dynamic Soft Admission Control*(DSAC) differs from *Static Soft Admission Control* (SSAC) because the former cooperates with power control in order to adjust power levels, so as to minimize power.

4.1.5 Load Estimation based Admission Control Algorithm

Similar to RPCAC/TPCAC approaches, the aim of a Load Estimation based Admission Control Algorithm is to admit, modify, or reject new RABs according to estimates of load, while respecting a pre-defined interference level limit, also called a Noise Rise threshold (T_{th}).
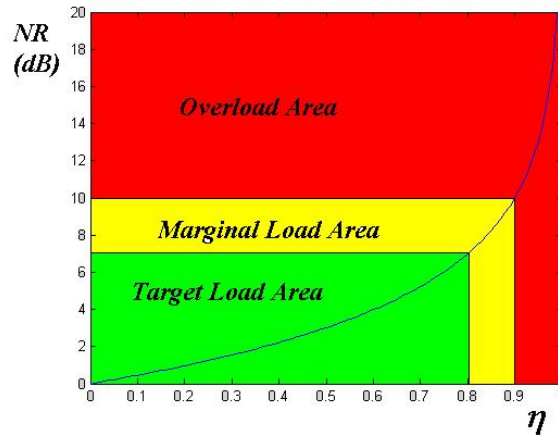
Figure 4.1: Noise Rise (T) vs. Cell Load (η)

This approach exploits the relation between Noise Rise (T) and Load (η), shown graphically in Figure 4.1:

$$T = \frac{P_{RX}}{P_N}, \eta = 1 - \frac{P_N}{P_{RX}} \Leftrightarrow T = \frac{1}{1 - \eta} \tag{4.1}$$

P_{RX} is the total power received at the BS, and P_N represents the constant Additive White Gaussian Noise power (AWGN).

Basically, load estimates are calculated based on the power gain measurements from all mobile stations in a certain area covered by a set of cells. These gain measurements can be obtained in two ways: from periodic requests of pilot power measurements to be executed by the mobile stations, or, from the handover candidates set for each mobile station, which remembers up to six of the strongest power gains, i.e. the six "strongest" cells.

Figure 4.1 shows three areas referred as *Target Load*, *Marginal Load*, and *Overload Areas*. Basically the first is the optimum operation area, and the third represents the area that Admission Control or other load control functions are trying to avoid. The Marginal Load Area represents a gap or headroom interval before a last resort action (in case none of the load control functions succeeded to maintain load levels under a predefined threshold). Noise rise violation is a term that denotes when the noise rise has passed a limit that would decrease the Quality of Service for currently served users.

Previous studies [23] indicate that for WCDMA systems *Load Estimation based Admission Control* best fits the Uplink case. This comes from the fact that the Uplink is interference limited, i.e., the Power/Noise Rise/Interference/Load are correlated quantities representing the main resource shared by the Uplink user.

4.2 Single-Cell Admission Control

As mentioned before, Admission Control algorithms are not standardized and several approaches have been proposed. The simplest one is a Single Cell (SC) case where the main admission criterion is the following condition (according to Figure 4.1):

$$T_{own} < T_{th} \tag{4.2}$$

where T_{own} is the noise rise at the concerned cell **after** the user has been admitted in the cell, as before T_{th} represents the noise rise threshold (indicating the onset of overload), which is defined according to the operator's network planning strategies.

Assuming that, in practice, it is impossible [21] to exactly predict the noise rise increase **before** the user is admitted and that power control algorithms are invoked, then the previous admission criterion can be restated as:

$$T_{own}^{est} = T_{own} - T_{hr} = T_{target} \tag{4.3}$$

T_{own}^{est} is an estimate of T_{own}, and T_{hr} is a "head room" parameter set to compensate for potential estimation errors, thus attempting to avoid T_{th} being reached. The same definition can be directly translated to a load threshold by making use of Equation 4.1.

T_{own}^{est} can be estimated as:

$$T^{est} = \frac{P_{RX} + \Delta P^{est}}{P_N} \tag{4.4}$$

Equation 4.1 can be rewritten as follows:

$$\eta_{own} = 1 - \frac{P_N}{P_{RXown}} \tag{4.5}$$

Which implies:

$$\Delta \eta = \frac{P_N}{P_{RX}} - \frac{P_N}{P_{RX} + \Delta P_{RX}} \tag{4.6}$$

However, we know from [18] that:

$$\Delta \eta = \frac{E_b}{W N_0} R \tag{4.7}$$

E_b) is the energy per bit, N_0 is the thermal noise density, W is the spread-spectrum bandwidth, and R is the user transmission rate.

Rewriting Equation 4.6 in function of ΔP_{RX} yields:

$$\Delta P_{RX} = \frac{P_{RX}^2}{\frac{P_N}{\Delta \eta}} - P_{RX} \qquad (4.8)$$

Equation 4.8 represents the additional power increase upon admission of a new call.

4.3 Multi-Cell Admission Control

Jose Carnero Oates [21] states that $\Delta\eta$ can be adapted for the multi-cell case, so $\Delta\eta_{serv}^{est}$ represents the fractional load increment at the serving cell, if it admits the new user, and is given by:

$$\Delta\eta_{serv}^{est} = w \cdot \frac{1}{1 + R_p(K) \cdot \frac{E_b}{N_o}} + (1-w) \cdot \frac{1}{1 + R_p(K) \cdot \frac{E_b}{N_o} \cdot \frac{P_N}{P_N + I_{neigh}}} \qquad (4.9)$$

W is the chip rate, $R_b(k)$ is the peak bit rate demanded by the user, $\frac{E_b}{N_o}$ is the required energy-per-bit to noise ratio, I_{neigh} is the wideband interference power from other cells, and w is the weight parameter which determines how much to overestimate or underestimate.

Assuming a perfect estimation of the load in the serving cell in Equation 4.9, and that load and noise rise are related to each other by Equation 4.1, we could apply this same estimate to the neighbouring cells by taking into account the following definition of coupling factor, and also using Equations 4.6 and 4.8. Let us consider Figure 4.2:
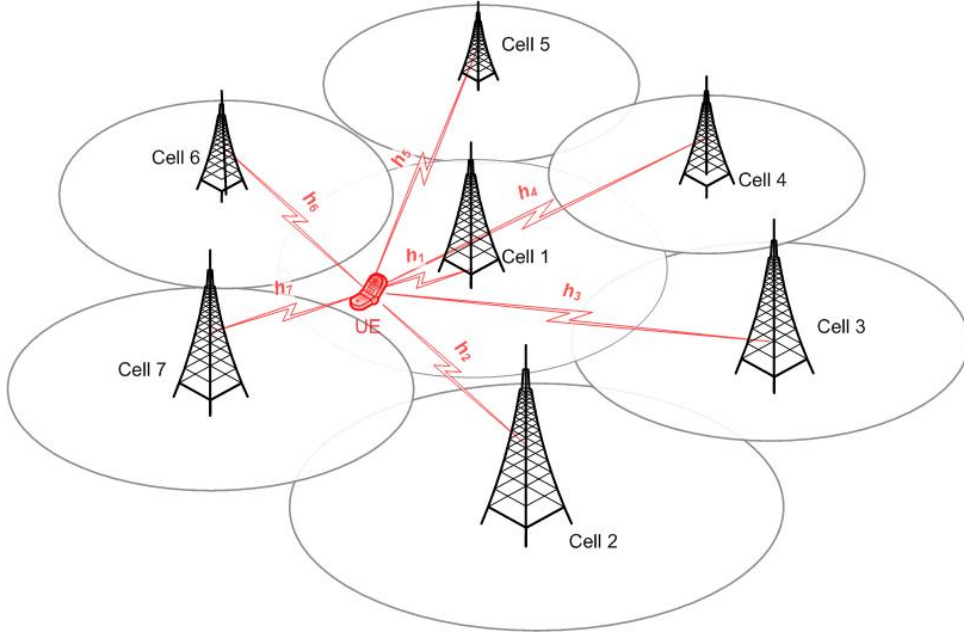
Figure 4.2: "7-cell-schema" with respective path gain factor h

We define the *coupling factor* "p" as the path gain ratio between one UE and 2 cells, one of these being the currently serving cell. In other words:

$$p_k^c = \frac{h_c}{h_{serv}} \qquad (4.10)$$

h_c is the path gain from mobile "k" to the cell "c" and h_{serv} is the path gain from the same mobile to the serving cell.

In real UMTS systems, these path gain parameters can be derived from pilot reports from the UE to the nearest cells; these measurements are available at the serving Node B. These reports provide information about the downlink path gain [19]. These parameters also provide us with a means to estimate the uplink path gains since Uplink and Downlink path gains generally only diverge because of fast fading. The UE signals and measurements are averaged over fast fading, it is reasonable to approximate the uplink path gain directly from the downlink (as derived from the pilot reports).

Based on this assumption, the pilot reports related to every link starting from a specific UE and terminating at a cell are described as follows:

$$\rho_c^{Pilot} = \frac{P_c^{Pilot}}{P_{RX}^{UE}} \tag{4.11}$$

ρ_c^{Pilot} represents the energy-per-chip to interference-power-intensity ratio E_c/I_o reported by the UE for the uplink cell "c", P_c^{Pilot} represents the pilot power transmitted by the same cell and P_{RX}^{UE} represents the total power received by the UE. Rewriting Equation 4.11 gives:

$$h_c = \frac{P_{RX}^{UE}\rho_c^{Pilot}}{P_c^{Pilot}} \tag{4.12}$$

It should be mentioned that P_{RX}^{UE} does not depend on the cell, since it is a downlink measurement and according to definition stated at Equation 4.11 it includes all the received interference, including the pilots.

Considering the previous definition of coupling factor and Equation 4.6 we can derive the fractional load increment of a given neighbour cell by:

$$\Delta\eta_{neigh}^{est} = \frac{P_N}{P_{RX}} - \frac{P_N}{P_{RX} + \Delta P_{RX_{serv}}p_k^{neigh}} \tag{4.13}$$

4.4 Approximate Capacity: Multi-Cell Case

Consider a set of $K = 1, \ldots, k$ best effort service classes, let us call $M(s)$ the number of current calls of class s which are active, and $M = (M(1), \ldots, M(k))$ the vector of number of active mobiles. Assuming a fixed number of mobiles, i.e., a fixed $\mathbf{M}$ is given, then Equation 4.14 indicates the power $P(s)$ required at the cell from a mobile $\in K$ [18]:

$$\tilde{\Delta}(s) = \frac{P(s)}{P_N + I_{serv} + I_{neigh} - P(s)}, s = 1, \ldots, k \tag{4.14}$$

N is the noise power, I_{serv} is the total power received from mobiles served by this cell, and I_{neigh} represents the total power received from mobiles within neighbouring cells.

$\tilde{\Delta}(s)$ represents the target ratio of the received power from a mobile of a certain class s to the total interference received at the cell, this can also be written as:

$$\tilde{\Delta}(s) = \frac{E(s)}{W N_0}R(s), s = 1, \ldots, k \tag{4.15}$$

$E(s)$ is the energy per bit (for a class s), N_0 is the thermal noise density, W is the spread-spectrum bandwidth, and $R(s)$ is the transmission rate for the class s service.

In this last equation we assume that the target ratio $(E(s)/N_0)$ does not significantly depend on the transmission rate $R(s)$. In [18], it can be seen that, over a wide range of rates, the maximum variation around the median value is less than 20%.

From Equation 4.14:

$$I_{serv} = \sum_{j=1}^{k} M(j)P(j) \tag{4.16}$$

In order to trace the relation between I_{serv} and I_{neigh} we can obtain from measurements [9] that, approximately:

$$I_{neigh} \cong i \cdot I_{serv} \tag{4.17}$$

Considering $\Delta(s) = \frac{\tilde{\Delta}(s)}{\tilde{\Delta}(s)+1} \Leftrightarrow \tilde{\Delta}(s) = \frac{\Delta(s)}{1-\Delta(s)}$, Equation 4.15 becomes:

$$\Delta(s) = \frac{P(s)}{P_N + I_{own} + I_{other}}, s = 1, \ldots, k \tag{4.18}$$

Solving the previous set of k equations (from Equation 4.18) yields

$$\Delta(s) = \frac{N \cdot \Delta(s)}{1 - (1+i)\sum_{j=1}^{k} M(j)P(j)} \tag{4.19}$$

The pole capacity, characterized by infinite required power for a certain class s, can be defined as the set M^* of vectors in $\mathbf{M}$, which makes the denominator in Equation 4.19 vanish, i.e.:

$$M^* = \{\mathbf{M} : \mathbf{1} = (1+i)\sum_{j=1}^{k} M(j)P(j)\} \tag{4.20}$$

One can change the previous definition in order to consider that $M(j)$ are actually integers (since $\boldsymbol{M}$ belongs to N^k)

Given the previous equations and $\boldsymbol{M}$ is the finite set of N^k where

$$1 > (1+i)\sum_{j=1}^{k} m(j)\Delta(j) \tag{4.21}$$

and,

$$\eta = max(1+i)\sum_{j=1}^{k} m(j)\Delta(j) \tag{4.22}$$

Altman defines the Integer Capacity $\boldsymbol{M}_B$ of the system as the boundary of $\boldsymbol{M}$ in which any new admitted call would lead to infinite power in Equation 4.19 [9].

His definition below follows from [22]:

Def: The blocking set $\boldsymbol{M}_B^j$ of class $j \in K$ is defined as the subset of $\boldsymbol{M}$ for which another call from class j cannot be accepted, i.e. $m \in \boldsymbol{M}_B^j$ if and only if

$$m \in \boldsymbol{M}, m + e_j \notin \boldsymbol{M}, \tag{4.23}$$

e_j is the unit vector in direction j.

4.5 Exact Capacity for a fixed number of mobiles: Multi-Cell Case

The problem with such a previous approach is the existence of the parameter "i", which implies an uncertainty about the relation between mutual interference between two or more neighbouring cells.

The previous model, precisely described by Equation 4.14 can further be interpreted as:

$$\Delta(k) = \frac{P_k}{P_N + \sum_{serv} M_k P_k + \sum_{others} M_k P_k p_k^{serv} - P_k} \tag{4.24}$$

Here $\sum_{others} M_k P_k P_k^{serv}$ represents I_{neigh}, where p_k^{serv} is the *coupling factor* between a "neighbouring mobile" and the serving cell, P_k is the power of a group-k user, and M_k is defined as the *group of users* in the set of UEs which have the same *coupling factor*. Similarly, $\sum_{serv} M_k P_k$ represents I_{serv}, i.e. the total interference received from the mobiles that belong to the serving cell. Thus, the approximate capacity can be rewritten, where $\boldsymbol{M}$ is the finite set of N^k such that:

$$1 > (\sum_{serv} M(k)\Delta(k) + \sum_{others} M(k)\Delta(k)p_k^{serv}) \tag{4.25}$$

and

$$\eta = max(\sum_{serv} M(k)\Delta(k) + \sum_{others} M(k)\Delta(k)p_k^{serv}) \tag{4.26}$$

Again, the Integer Capacity is defined as the boundary of the polyhedron of system states that makes the solution P_k for Equation 4.19 tend to infinity in case of a new arriving call.

4.6 Admission Control and Elastic Traffic

As it has been shown, interference is the main resource in the uplink, hence this interference has received much attention. Most radio resource management investigations today aim to provide better services by parsimonily using resources. However, the data rates for uplink channels in the next releases of UMTS will reach approximately 5Mbps, thus making radio resource management a very important issue, but perhaps offering new possibilities.

In this context we must define *elastic traffic*. 3GPP classifies traffic patterns into 4 types (as described in Section 2.6). The usual demands in a multi-service system can be classified in the most general case into two broad categories: "streaming" and "elastic". Where streaming traffic includes both real-time conversational traffic (voice and video) and downloaded audio and video sequences, it is characterized by a requirement on the network to rigidly respect some predefined QoS requirements such as low loss and bounded delay. Elastic traffic, on the other hand, corresponds to the transfer of all forms of finite sized objects (files, web pages, MP3 ...) and is called elastic because the transmission rate can be rather freely adjusted depending on competing network load. Quality of service requirements for elastic traffic are typically given in terms of response times (typically in the range of seconds, rather than the delay bounds for streaming traffic which are in the range of 10s of seconds to hundreds of milliseconds). The essential traffic characteristic of a streaming flow is its (generally variable) bit rate, while an elastic flow is characterized more simply in terms of its total size.

Recent results have shown that the Erlang capacity of CDMA networks increases when the elasticity of the traffic carried increases, in the sense that the transmission rates of the elastic traffic are allowed to be slowed down [9] (see also [7] and [8]). This conclusion is not immediately evident since slowing down the transmission during a session necessarily increases its holding time. This holding time can increase indefinitely until it reaches a "time-out" value, which will eventually lead to a dropped session.

4.6.1 Slowdown feature for elastic sessions

Recall that $\Delta(s)$ depends directly on the required bit-rate. Elastic services that are explicitly rate controlled can tolerate a certain slowdown of their peak bit rate $R_p(s)$ as long as its slowed down instantaneous bit rate remains greater or equal to a minimum required bit rate $R_p(s)/(s)$, which represents the *guaranteed bit rate* (GBR) associated with the user class. In the case that a user of class s has its bit rate slowed down to $R_p(s)/a(s)$, and its new required target ratio $\Delta_a(s)$ becomes:

$$\Delta_a(s) = \frac{\tilde{\Delta}(s)}{a(s) + \tilde{\Delta}(s)} = \frac{\Delta(s)}{a(k)(1 - \Delta(s)) + \Delta(s)}, s = 1, \ldots, k \qquad (4.27)$$

The previous equation describes the relationship between the class-wise slowdown factor $a(s)$ and its respective target ratio $\Delta_a(s)$. This definition is essentially theoretical and will be adapted in the following sections to best represent it as a reasonably heuristic model that will be implemented in the simulator CASPER, as described in Chapter 6.

4.6.2 The Uncoordinated Slowdown Mechanism

In brief, the slowdown technique reduces the session bit rate if the current cell load is over a predefined load limit defined as the *Load Target* (η_{tg}). From Section 4.2 we learned that the *Noise Rise Threshold* (NR_{th}), or better the reciprocal *Load Threshold* (η_{th}), is the decision parameter that indicates if a new arriving call should be rejected or admitted into the system considering the admission decision algorithm applied. If we consider a rate control mechanism based on current load situations, such as the slowdown mechanism, the *Load Target* is necessary due to the large variations of the Noise Rise. Both the Load Target and Load Threshold create a *headroom gap* which is denominated as *Marginal Load Area*. In other words, the Equation 4.27 that was previously described as class-wise becomes now a session-wise equation, i.e. regarding individually each user and not a class of users.

$$\Delta_a(i) = \frac{\tilde{\Delta}(i)}{a(i) + \tilde{\Delta}(i)} = \frac{\Delta(i)}{a(i)(1 - \Delta(i)) + \Delta(i)}, i = 1, \ldots, N \qquad (4.28)$$
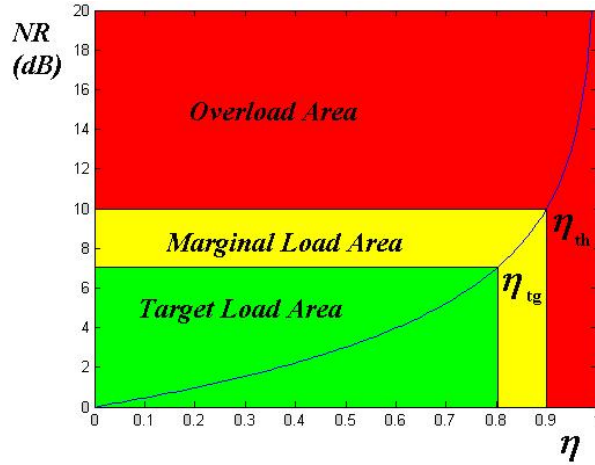
Figure 4.3: Load Target and Threshold limits

In Equation 4.3, if we consider a 7-cell-system the Uncoordinated Slowdown mechanism will work as follows (see Figure 4.4):

1. In the beginning of the *Time to Transmit Interval* (TTI), all the users begin the slowdown process with their peak bit rates, even the ones that were slowed down in the previous slowdown. Each of the η_x is then calculated individually based on estimates from Equation 4.28 and Equation 4.18.

2. Each one of the 7 cell loads are individually compared according to the inequality $\eta_x < \eta_{tg}$

3. If one or more cells have their current load levels equal or higher than the Load Target, one random user has its bit rate slowed down. This random user is taken from the group of user with the highest bit rate, or even, with the largest number of transport blocks per TTI, i.e. one transport block less is offered to this specific user.

4. The new load levels are calculated individually for each cell, based on Equation 4.28 and Equation 4.18

5. This process repeats until the cell load estimated levels η_x have reached the target level or there are no more "slowable" users in the cell that is "*slowed down*"

It is important to indicate that, since it is a "*single-cell*" based mechanism, no consideration to other cells is taken in any of the steps just described. Since the interference is a shared resource for all cells, slowing down users simultaneously in two or more cells leads to a false slowdown, i.e. bringing cells to load levels further below the pre-intended target level (η_{tg}). This false slowdown could eventually impact the next slowdown process, meaning that the cells judge their load capacity erroneously when putting users back to their peak rates in the first step of the slowdown process, as described in step 1.
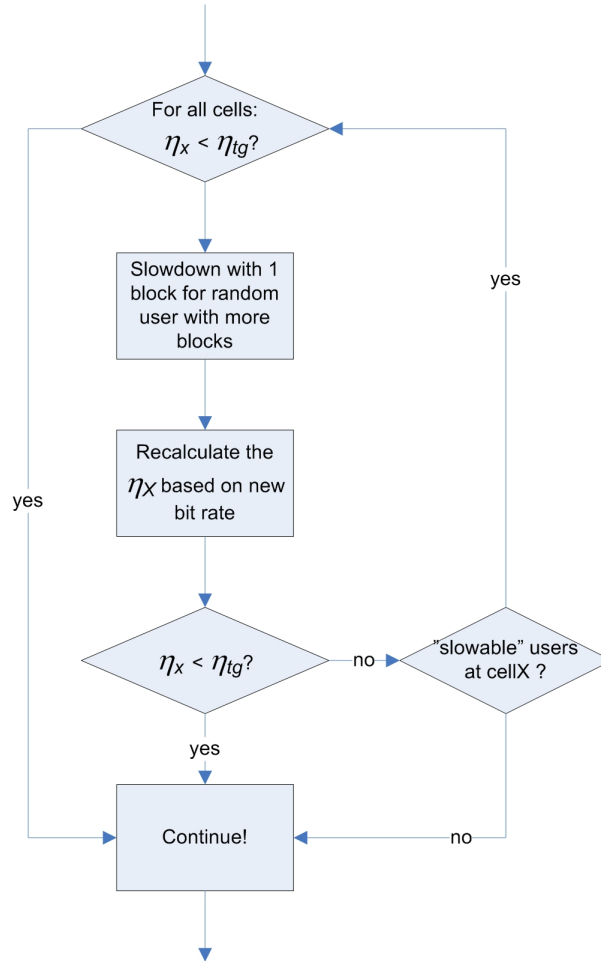
Figure 4.4: Uncoordinated Slowdown Mechanism

4.6.3 The Coordianted Unfair Slowdown Mechanism

The principle of which the Coordinated Unfair Slowdown technique consists is basically the same as described earlier for the Uncordinated case. However information from all cells is used together in order to accomplish a more refined and consistent slowdown process. For a similar 7-cell-system, the Coordinated Unfair Slowdown will happen as it follows (see Figure 4.5):

1. In the beginning of the *Time to Transmit Interval* (TTI), all the users begin the slowdown process with their peak bit rates, even the ones that were slowed down in the previous slowdown. Each of the η_x is then calculated individually based on estimates from Equations 4.28 and 4.18.

2. Each one of the 7 cell loads are compared according to the inequality $\eta_x < \eta_{tg}$

3. If one or more cells have their current load levels equal or higher than the Load Target, the cells are sorted in a descending order and one random user has its bit rate slowed down. This random user is taken from the group of user within that particular cell with the highest bit rate, or even, with the largest number of transport blocks per TTI, i.e. one transport block less is offered to this specific user.

4. The new load levels are calculated individually for each cell, based on Equation 4.28 and Equation 4.18. The slowed user bit rate has consequently automatically impact on all cell load levels.

5. This process repeats until all the cell load estimated levels η_x have reached the target level or there are no more "slowable" users in any cell.

Figure 4.5: Coordinated Unfair Slowdown Mechanism

4.6.4 The Coordianted Fair Slowdown Mechanism

The principle of which the Coordinated Fair Slowdown technique consists is basically the same as described earlier for the Coordinated Unfair case with the exception that one user can be slowed down twice only if all the other users from different cells have been slowed down one time. For a similar 7-cell-system, the Coordinated Fair Slowdown will happen as it follows (see Figure 4.6):

1. In the beginning of the *Time to Transmit Interval* (TTI), all the users begin the slowdown process with their peak bit rates, even the ones that were slowed down in the previous slowdown. Each of the η_x is then calculated individually based on estimates from Equations 4.28 and 4.18.

2. Each one of the 7 cell loads are compared according to the inequality $\eta_x < \eta_{tg}$

3. If one or more cells have their current load levels equal or higher than the Load Target, the cells are sorted in a descending order and one random user has its bit rate slowed down. This random user is taken from the group of user within that particular cell with the highest bit rate, i.e. one transport block less is offered to this specific user.

4. The new load levels are calculated individually for each cell, based on Equation 4.28 and Equation 4.18. The slowed user bit rate has consequently automatically impact on all cell load levels.

5. This process repeats until all the cell load estimated levels η_x have reached the target level or there are no more "slowable" users in any cell.

6. Users are then fairly slowed down, meaning that all users in the system are provided with X or X-1 blocks, given that $\frac{8}{\tilde{a}} < X \leq 8$.
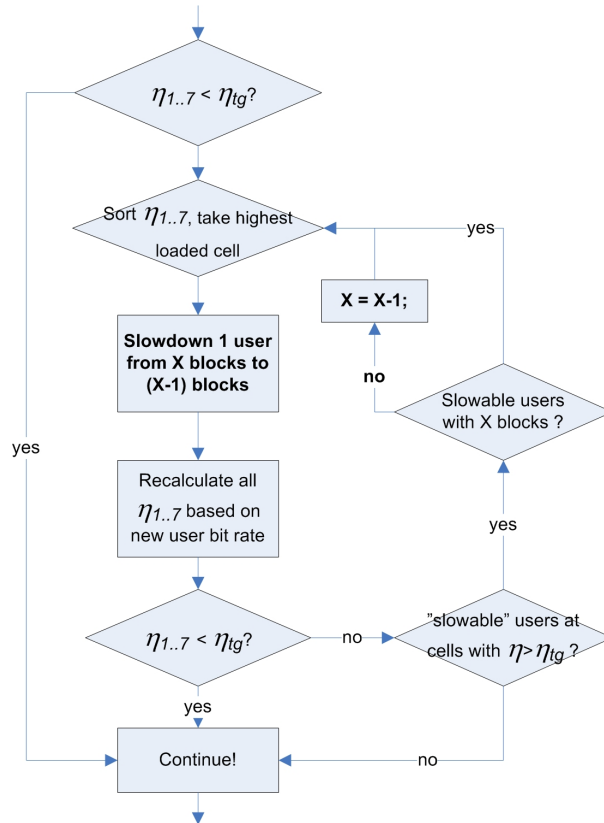
Figure 4.6: Coordinated Fair Slowdown Mechanism

4.7 Summary

This chapter presented a main purpose a deep analytical description of the two key aspects of this thesis: Admission Control and Rate Control (slowdown) mechanisms. Basically, it showed how information from

several cells can be used for the purpose of improving system capacity and avoiding false accepts that could lead to lower provisioning of quality of service. Related models were conveniently presented, next we will adapt such functions into a WCDMA simulator.

Chapter 5

Problem Statement

5.1 Earlier Work

CDMA teletraffic has been topic of radio resource management research since it started to gain popularity in military and commercial applications. Several are the techniques to apply admission control as a load control function are described below.

Jose Outes [21] compares Multi-cell vs. Single-cell Admission Control in two different load cases. In the first case, he considered a seven-cell-environment, with cells being homogenously loaded with users, and in the second case non-homogeneously. The three main conclusions from his works were:

- Unlike the homogeneous load case, a significant capacity increase occurs under non-homogeneous conditions in comparison to a single-cell scheme, for both low and high data rate users.

- A Multi-cell Admission Control Algorithm leads to a significant reduction in the probability of Noise Rise violation in the adjacent cells, due to erroneous admissions in the serving cell. This enables an increase in the Admission Control decision threshold, assuming the same target blocking probability.

- Multi-Cell Admission Control is more conservative than Single-Cell Admission Control, meaning that more rejections are made when making the admission decision, which implies that the Multi-cell Admission Control makes fewer admissions, leading to less dropping of established connections.

Jose Outes conclusions are important but did not consider the impact of elastic traffic in admission control functions, nor did he consider the impact of Admission Control on the system's overall performance.

Altman proposed a method to calculate the class-wise blocking probabilities as functions of the estimated inter-cell coupling factors [9]. Basically, this method assumes that the Admission Control entity knows exactly the path gain factor between mobiles and every cell. An important assumption is that perfect power control is assumed. In order to get these blocking probabilities a set of k equations needs to be solved (Equation 4.18).

Fodor gives an exact solution for this set of equations in [14]. His approach adapts the approximation regarding the relation between the internal and external interference, i.e. the "i" factor, considering the "*individual interference*" generated by neighboring mobiles. Fodor's studies present a more analytical model of Multi-Cell Admission Control. In both [14] and [9], session drop and uplink block error probability were not taken into account.

Fodor and Telek have presented some important performance analysis of elastic sessions in an Uplink CDMA cell [15]. A relevant conclusion from their work is that there is a clear need to establish bandwidth sharing policies for multiple elastic classes, which may have a strong impact on the final throughput, and consequently on the session holding times. The two simple policies adopted in their paper revealed that such policies did **not** impact blocking probabilities. Such bandwidth sharing policies are a part of scheduling algorithms. However, analysis of general *Scheduling Algorithms* (SA) for the uplink goes

well beyond the scope of this thesis and hence is not part of my simulations. Despite this, both uplink scheduling algorithms and Admission Control algorithms are inter-related and as such are both relevant.

In contrast to the above references, which avoided some points and had a more theoretical approach, this thesis aimed to provide theoretically important and practically useful insights in order to analyze the performance of Multi-cell over Single-cell admission control algorithms. The study also considered the impact of other transversal radio resource management functions, such as the rate control and power control functions.

5.2   Problem Statement and Solution Approach

As is clear from the previous sections, Uplink Admission Control has become a more important issue due to the increasing throughput demands upon the Uplink channels. Previously cellular traffic used to be predominantly constant bit rate voice calls, but with the addition of new services the uplink channels have recently become more "*bursty*" with long-tailed traffic. In this sense, decision algorithms, which control admission/rejection of new arriving sessions into a cellular system, need a more thorough analysis in order to evaluate how these algorithms impact the overall system performance.

5.3   Methodology to Evaluate the Proposed Solution

This research utilized simulation to clarify these *dependencies* and *trade-offs* between some key measures in Admission Control, such as session-wise throughput, system throughput, block error probability, dropping and blocking probabilities, the system's Erlang Capacity, and inter-cell interference factors. All these measures are considered in a multi-cell WCDMA environment with convenient admission control and fair sharing policies provided by the existing pertinent scheduling algorithms.

Particularly the dropping and blocking probabilities are analyzed together with the system throughput. This trade-off analysis is of greater relevance given the 128kbps elastic user class since rigid traffic results clearly indicate a final throughput dependents primarily on the total number of users served by the system. Considering that session dropping is perceived negatively by end users, in fact more negatively than blocking a session, thus the dropping probability results are particularly important in Admission Control mechanisms. This is due to the fact that one can reduce the dropping probability by using more conservative RRM techniques, including Admission Control at the expense of increasing the overall blocking probability. The trade-off between throughput, blocking probability, and dropping probability should be then analysed as a function of the RRM functions such as: Admission Control, Power/Rate Control, and Dropping Control. The simulations are intended to elucidate such dependencies (see Figure 5.1).
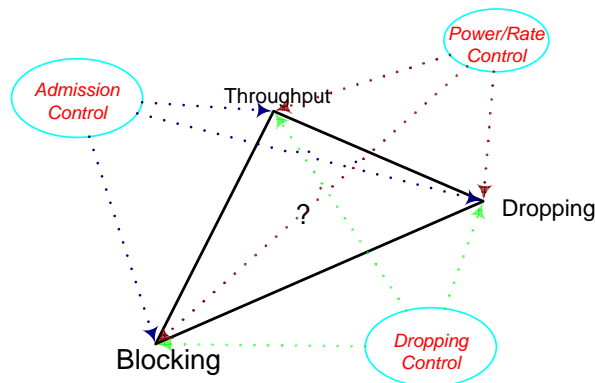
Figure 5.1: Trade-off: Throughput, Blocking and Dropping

These simulations utilized Casper [25], a WCDMA simulator running on Matlab [3]. Given a set of parameters concerning radio propagation, base station settings, user equipment settings, and traffic, the software generates and handles traffic in a simulated WCDMA network.

Some code modifications to Casper were needed in order to implement the Single and Multi-cell Admission Control algorithms, as well as for the slowdown mechanisms.

This page intentionally contains only this sentence.

Chapter 6

Simulation Model

The primary goal of this chapter is to briefly expose the simulation model employed in order to help the reader understand how the analytical model presented in Chapter 4 was adapted for the simulation purposes. No consideration in order to analyze the simulator was explicitly intended.

6.1 Propagation Model

The propagation model is characterized by an extensive set of channel qualities that reflect the propagation model, mainly expressed as attenuation. This attenuation (also called "pathloss") is the inverse of the path gain. The path gain, h, is thus the ratio of the received power to the transmitted power and it consists of four different parts,

$$h = h_a + h_d + h_s + h_m < 1 \tag{6.1}$$

Here, h_a is the antenna gain, h_d is the attenuation due to distance, h_s is the shadow fading, and h_m is the multipath fading. The antenna gains and distance attenuations are input as lookup tables. The lookup table describing distance attenuation is calculated using to the Okumura-Hata model [17]. Because the system users are not mobile, fast fading is therefore modeled as zero. User mobility was disabled in order to better verify the impact of admitted calls on the system, by decreasing load variations due to users moving from cell to cell.

As described by the Equation 4.10, the path gain is fundamental because it serves as basis to calculate the coupling factor.

6.2 Simulation Scenarios

The simulation scenarios should be chosen such that the simulations reflect a realistic situation. On the other hand, a perfectly realistic model is impossible to implement. Also, adjustments and simplifications have to be made to avoid excessively complicated calculations and excessive logging. The simulation scenarios were chosen as a compromise between a realistic and a feasible simulation.

6.2.1 Traffic Model

An important issue in designing any simulation is a clear definition of service classes to be adopted. Although 3GPP standards for UMTS envisage four different service classes: conversational, streaming, interactive, and background; as explained at Section 2.6, for the purposes of my simulations only two traffic classes will be considered: streaming and elastic traffic. According to Roberts [24], the essential distinction between streaming and elastic traffic is that the former requires open loop control while the latter is most efficiently handled using closed loop control. He says that, under open loop control,

admission control is applied in order to admit streaming flows while providing the proper quality of service.

In this sense, bufferless multiplexing represents the most satisfactory form of statistical multiplexing, facilitating control with good performance. However, he also goes on to say that this kind of multiplexing becomes inefficient for systems such as UMTS that are buffered by nature. In any case, our primal goal was to exploit the distinction between the streaming and elastic traffic, and to understand their dependencies on admission control algorithms. Four types of users are considered:

Voice with duplex transmission with Discontinuous Transmission (DTX) at 12.2 kbps in dedicated channels.

Video with simplex at 64 kbps in dedicated channels

UL128 (kbps) with simplex transmission at 128 kbps in dedicated channels

Despite the DTX function, Voice and Video users are considered as a rigid traffic model, i.e. with a constant bit rate, while the UL128 users are modeled as elastic traffic, i.e., allowed to have their bit rates changed according to the description of the slowdown functions described at Sections 4.6.2, 4.6.3, and 4.6.4.

6.2.2   User and Data Creation

Users are added to the system following a *"batch arrival"* process that emulates a Poisson process. This process is described briefly below.
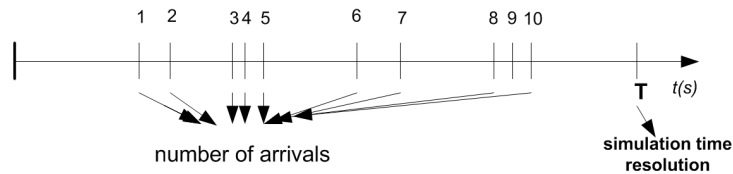
Figure 6.1: Batch Arrival Schema

Since a genuine Poisson process happens in a continuous time basis, the Batch Arrival Process emulates a Poisson behavior on a discrete time basis. The simulator is a Discrete Time Event Simulator. During a time **T**, arrivals occur in accordance with an exponential distribution, and with a specific session arrival intensity λ. It is important to mention that this Poisson emulation creates two main issues:

Busy period - when within one time step, a call could have come and left the system, then the simulation would not have kept track of this arrival or departure.

Batching - a call comes to the system within a time step, but there is not sufficient time for it to interact with the system, for example to change rate and change transmission power.

If we consider the simulation time steps to be short enough (in Casper the time step is 10ms), the effects of these two problems should be irrelevant, since the simulation is done for a very long duration (around 100,000 time steps) basis, which yields a very acceptable "Poisson-discrete simulation".

From Little's formula, the expected total number of users in a $(M\|M\|\inf)$ queuing system is:

$$N = \frac{\lambda}{\mu} \tag{6.2}$$

Where μ stands for the session departure intensity, or the inverse of the session mean holding time, and λ stands for the session arrival intensity.

For packet users, a mean packet size is defined by an exponentially distributed function [25], which will in turn impact the holding time for a specific session.
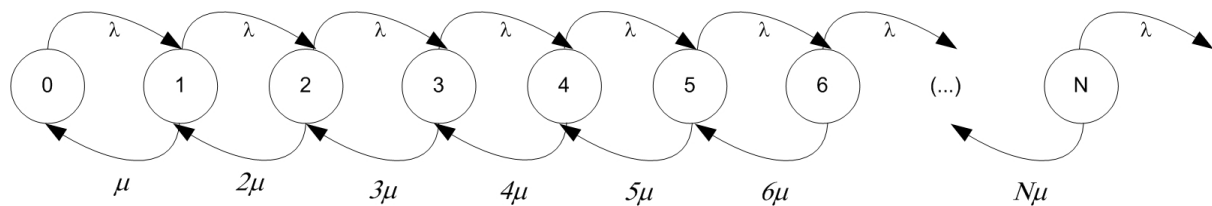
Figure 6.2: Arrival and departure procedures in a $(M\|M\|\inf)$ queuing system

6.2.3 Cell Deployment

Simulations were done in a 7-cell-environment. Sites are laid out in a uniform hexagonal pattern, with omni directional antennas. A default wrap-around technique is used.

6.2.4 Cell Load Deployment

In order to create different load situations, users should or should not be born into different cells.

Load Case 1 - **Homogenous** Case
In a multi-cell environment, users are placed with equal probability in a cell.
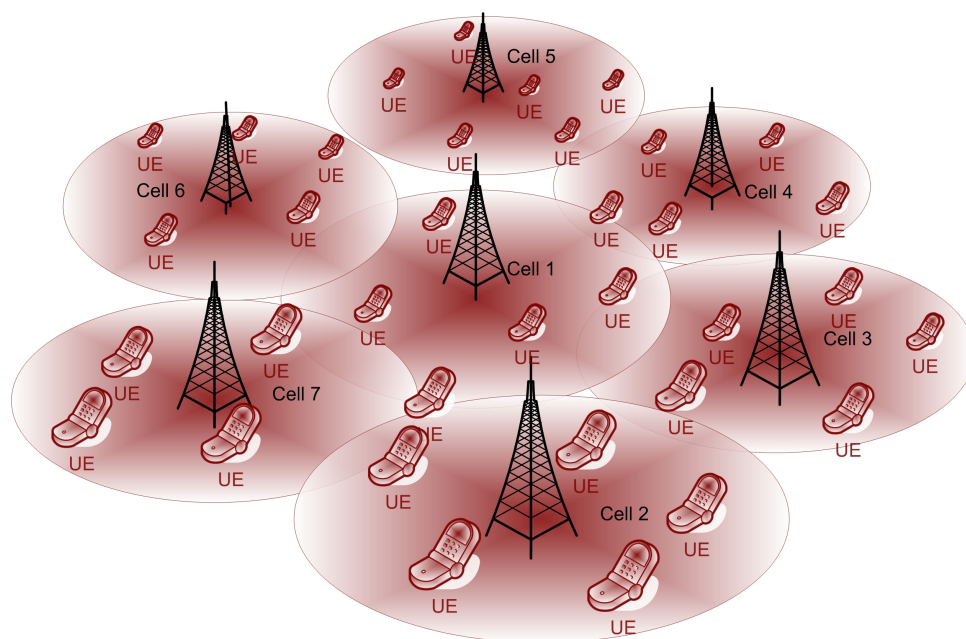
Figure 6.3: Homogeneous Load Case

Load Case 2 - Heterogeneous **Hotspot** Case
In a multi-cell environment, users are placed with higher probability (75%) into the central cell.

Load Case 3 - Heterogeneous "**Hotround**" Case
Basically the opposite of the previous case. Users are placed with higher probability (95%) into the neighbor cells to the central one.
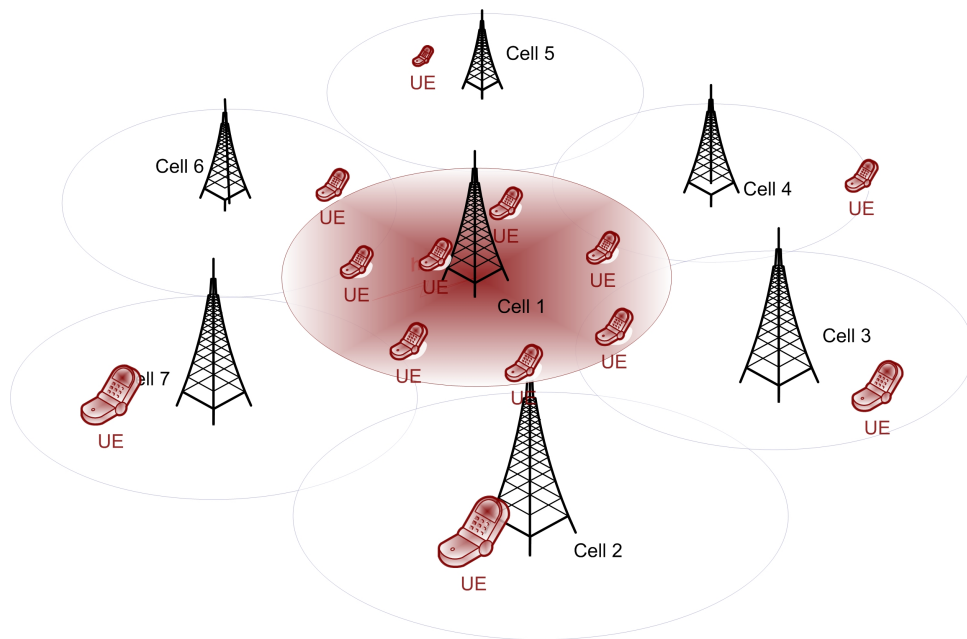
Figure 6.4: Heterogeneous Hotspot Load Case
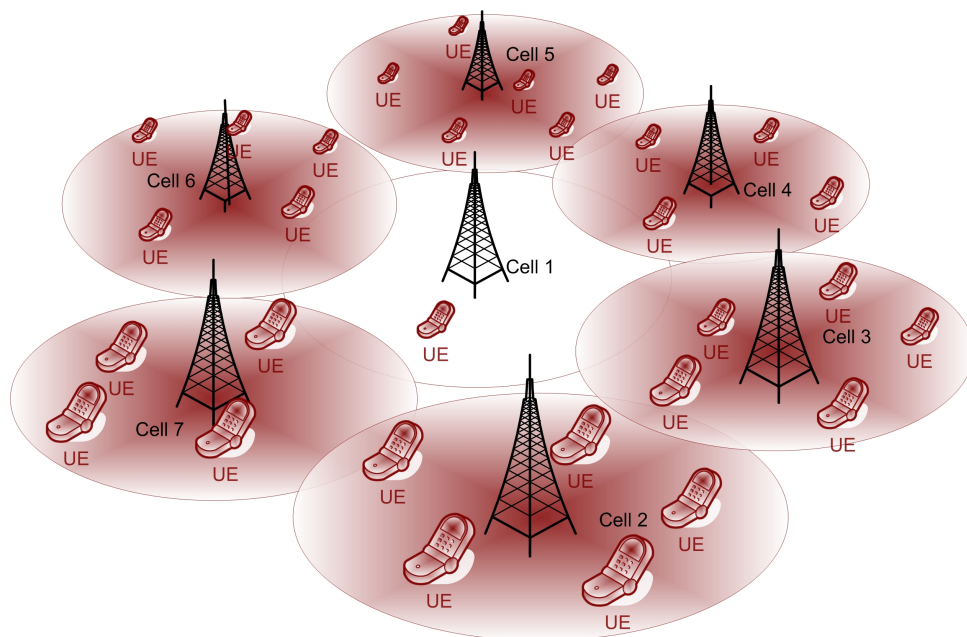
Figure 6.5: Heterogeneous Heterogeneous Load Case

6.3   System Model

6.3.1   Power Control

The power control is based on the inner and outer loop power controls. The former compares the received SIR with the target one. The transmission power is then increased by 1dB if the received SIR is below

the target, and decreased by the same amount if the received SIR is above the same target.

The outer loop controls the target SIR. The target SIR is increased by a fixed step for each erroneously received block, and decreased by a smaller amount for every correctly received block. The ratio between the increase and decrease amounts is calculated based on the block error rate (BLER) target, such that the actual BLER, in a stationary situation, will converge to the BLER target.

6.3.2 Rate Control

Rate Control occurs once in every radio frame for every user. The algorithm sets the number of transport blocks to fit all buffered data, or to the maximum allowed value. After this rate selection, the transmitted power and the carrier-to-interference ratio are adjusted to fit with the new rate.

An additional slowdown rate feature implemented in the simulator is further described in Sections 4.6.2, 4.6.3, and 4.6.4.

6.4 Simulation Logging

Each scenario was previously simulated multiple times with different simulation times in order to check for results consistency. Considering my observations, the simulated time was then set to 1000 seconds, and the logging starts after 5 to 10 seconds when the traffic is assumed stable. Before these time, there is also a period called "slowstart" that lasts 100ms. The mean holding times are in average 2s (for voice and video) and in average 3.3s (for UL128). After 5 to 10 seconds, a large number of users created during the slowstart phase have already left the system, and final results were verified to not longer be affected. The logging happens every 10 milliseconds, and keeps tracks of repetitive and non-repetitive events, the later in an event-driven basis. In the Appendix the reader can find a table referring to the respective confidence intervals of every data used to plot graphics illustrated in this Thesis work.

6.5 Description of Simulation Parameters

For a good understanding of results it is important to present some of the simulation parameters that served as input, and consequently affect the outcome of the simulations. We define as one simulation a set of experiments that has as a main outcome the outputs defined below, representing one curve in a plot.

Inputs:

- **Uplink Load Threshold** (η_{th})- the threshold for the Admission Control decision

- **Uplink Load Target** (η_{tg}) - the value that the Slowdown algorithm utilizes as the reference value that the Slowdown process aims at.

- **Lambda** (λ) - the arrival intensity of users into the system, which during one simulation is increased in specified percentages from the initial for every experiment.

- **Maximum Slowdown Rate** ($\hat{a}$) - how many times the peak bit rate for a UL128kbps user can be slowed down.

Outputs:

- **Blocking Probability** (β) - the probability of blocked calls due to Admission Control during one experiment.

- **Uplink Block Error Probability** (ULBLEP) - the ratio of the number of incorrectly received blocks to the total number of blocks transferred in the Uplink.

- **Dropping Probability** - the probability of dropped calls due to Congestion Control Algorithms during one experiment. In other words, one call is dropped when its uplink block error probability overpass a pre-defined threshold.

- **Average Number of Users** (N) - the average number of users in the system, i.e., how many users are present in the system on average during the entire simulation.

- **Mean Uplink Load** - the average Uplink load during one experiment.

- **Mean Throughput** - the average of bits successfully transmitted in the Uplink per second during one experiment.

- **False Accepts Probability** (FA) - the probability of occurrence of an admitted call into the system, when one or more of the neighbouring cell loads are higher than η_{th}. This probability is valid only for the Single-cell Admission Control algorithm.

The parameters above are used as input or are outputs of the entire system (seven cells). The parameters in Table 6.1 were used in all cells, unless otherwise mentioned.

Environment models / parameters	**Value**		
Cell Radius	500 meters		
Site Deployment	1-sector-site		
Number of Cells	7		
Chip rate	3.84 Mchips/s		
Base Station Antenna	Omni directional		
Pathloss	L = 29.03+3.52log(d), d = distance [m]		
Fast fading	3GPP Typical Urban		
Shadow Fading	Log/Normal, σ = 8dB Correlation distance : 100m Correlation, one MS to different BS: 0.5		
Maximum Transmission Power in the Uplink	21 dBm		
Minimum Transmission Power in the Uplink	- 50 dBm		
Thermal Noise Level in Uplink	- 135.85 dBm		
Thermal Noise Level in Downlink	- 129.157 dBm		
Fast PC step size	1dB		
Traffic Models/Parameters	*Voice*	*Video*	*UL 128kbps*
Average User Speed	0 m/s		
Initial Uplink SIR Target	0.0075	0.0224	0.0405
Mean Packet Size	-	-	50 kbytes
Mean Holding Time	2s	2s	-

Table 6.1: Overall Simulation Parameters

Chapter 7

Simulation Results and Analysis

As described earlier, we have considered 3 scenarios with 3 different user classes, two based on a rigid traffic (voice and video), and the third elastic, which means variable bit rate as controlled by the slowdown mechanisms (described in Sections 4.6.2, 4.6.3, and 4.6.4). The first scenario is based on a homogeneous load case, i.e. users arrive in any of the 7 cells with equal probability, while the 2nd and the 3rd represent the heterogeneous load case: "hotspot" and "hotround", respectively.

The second and third scenarios were not applied to the 3rd user class, i.e. the 128kbps elastic upload traffic model. Their results were not of significance due to the fact that they follow the same pattern as the voice and video classes.

Basically the simulations input were: the three scenarios, the three user classes, the parameters described in Chapter 6, and the Single-Cell and Multi-Cell Admission Control algorithms associated with the respective Uncoordinated and Coordinated slowdown mechanisms. Simulation using these inputs generated a series of graphics illustrating mainly the class-wise blocking and outage probabilities, false accepts, noise rise violation probability, uplink and downlink blocking error probability, as well as system and mean user (*session wise*) throughputs.

7.1 Voice Users

The primary goal of these simulation scenarios concerning the voice class was to show performance comparisons between Single-cell (SC) and Multi-cell (MC) Admission Control Algorithms for different traffic models. Table 7.1 summarizes the specific simulation parameters.

Admission Control	Users	Load Case	η_{th}	$\lambda_{initial}$ ++ increment
SC	Voice	Homogeneous	0.75	210++10%
MC	Voice	Homogeneous	0.75	210++10%
SC	Voice	Hotspot	0.75	56++8%
MC	Voice	Hotspot	0.75	56++8%
SC	Voice	"Hotround"	0.75	210++10%
MC	Voice	"Hotround"	0.75	210++10%

Table 7.1: Simulation Parameters for Voice Users

7.1.1   Homogeneous Load Case

The homogeneous load case results indicated that the Multi-cell Admission Control started to be significant when the session arrival intensity $\lambda \geq 240$ *persecond* (see Figure 7.1(a)). The blocking probability difference is between 0% and 3%. Even though the blocking probability difference does not increase after λ=293(*persecond*) ($\beta = 0.06$ and 0.04), it is interesting to notice that the outage probability seen in Figure 7.1(b) is affected, with Figure 7.1(c) confirming a similar outage as a function of the number of current users (admitted) in the system. From these two last figures, the presence of two regions should be noted, (1) the slope λ¡300(1/s)) indicating an increasing outage probability, and (2) a slight "platform" λ¿300(1/s)) indicating that little change in ULBLEP and DLBLEP contributes to outages in MC and SC cases. This implies that the Admission Control load control function is more significant than the Dropping load control function. Figure 7.2 provides an DLBLEP results as foundation to this conclusion.

Analysing further Figure 7.1(d), we note an improved uplink block error probability (ULBLEP) in the order 0% to 3.1%, which is even more pronounced in Figure 7.1(e) that shows ULBLEP as function of the current number of users in the system, with a gain ranging from 0% to 7.5%. As indicated previously, the influence of the downlink traffic can also be noted, as one can see that for $\lambda > 357$(*persecond*) the ULBLEP tends to increase again - this is due to the fact that downlink related outage probability is not significantly increased. Figure 7.1(f) illustrates the false accepts probability for the Single-Cell Admission Control case.

7.1.2   Heterogeneous Hotspot Load Case

Comparing Figures 7.3(b), and 7.3(c), a significant difference in blocking probability can only be seen for new arriving calls in the neighboring cells, which in turn slightly affects the system overall blocking probability difference between the Single and Multi-Cell Admission Control cases (Figure 7.3(a)). These results were clearly as expected considering that the weight factor for these simulations was purposely set to 1, which makes the Multi-Cell AC behave as Single-Cell-based, in the case of all calls arriving in the central cell, which would be a "100% Hotspotly" loaded situation. Similarly it can be seen comparing Figures 7.3(f) and 7.3(c), there is slightly higher blocking probability in the Multi-Cell case than the false accepts probability in the neighboring cells.

With regard to the Heterogeneous Hotspot load case, the results could be seen as less clear than those obtained from the Homogeneous load case. However, it should be remarked that in order to maintain stability in hotspot scenarios, especially in the "hotspotted" cell, the η_{th} should be set to lower values (around 0.15, see Figure 7.4), which would make the Single-Cell Admission algorithm reject the false accepts in the neighboring cells, thus decreasing the noise rise violation in the "hotspotted" cell. Although no simulations were done explicitly to examine this case, it seems evident that decreasing η_{th} to approximately 0.15 is the only way to decrease the occurence of false accepts in the central neighbor cells, thus decreasing the noise rise violation probability. However, by setting a much lower uplink load threshold η_{th} for all 6 neighboring cells results in as a large waste of capacity.

Interestingly, Figure 7.3(d) shows that the outage probability for users served by neighboring cell decreases with Multi-Cell Admission Control, due to its more conservative behaviour in admitting new calls, while the Single-Cell case yielded a constant outage probability $\approx 1,7\%$.

7.1.3   Heterogeneous Hotround Load Case

Results obtained from the Heterogeneous Hotround load case simulations lead to similar conclusions when compared to those from Section 7.1.1. Uplink block error probability and outage probability differ when one compares results from the hotround and central cells. Figure 7.5(e) implies that users wrongly admitted with the Single-Cell admission control start to encounter increasingly more outage events from λ=14.7(*persecond*), while Multi-Cell admission control keeps the outage probability around 5%. Considering that most users are actually located in the neighboring cells, we expected to see similar results in Figures 7.5(d) and 7.5(f), as in fact we see.
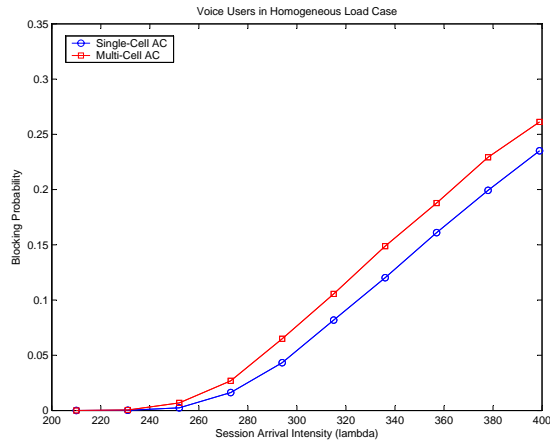
(a) Overall Blocking Probabilitiy
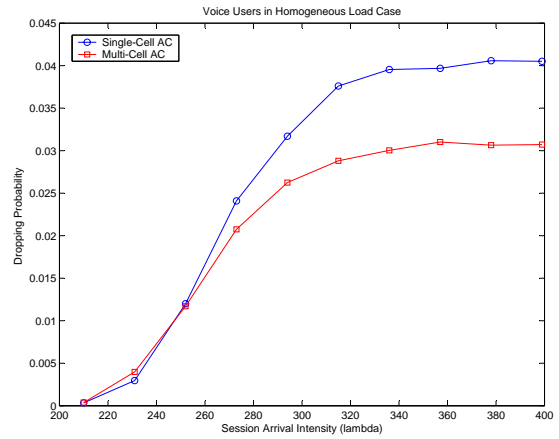
(b) Overall Dropping Probability
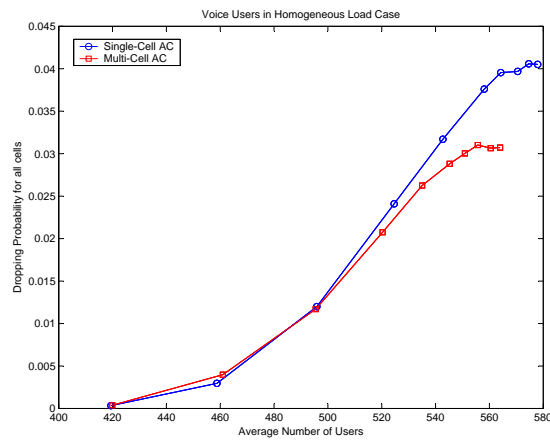
(c) Overall Dropping Probability - f(users)
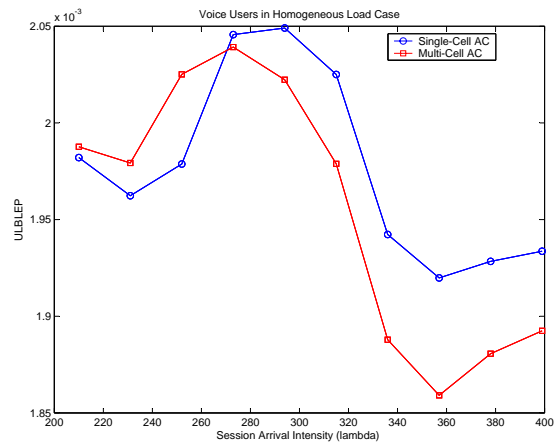
(d) Overall ULBLEP
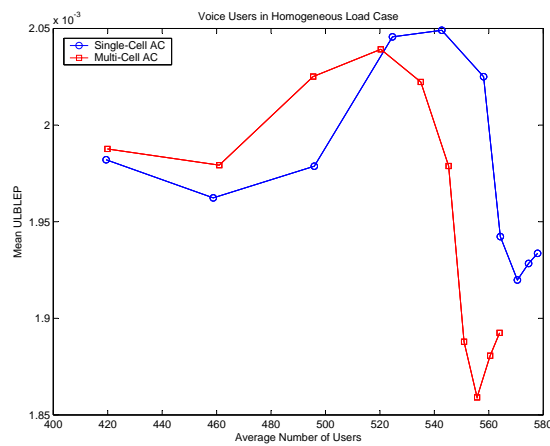
(e) Overall ULBLEP - f(users)
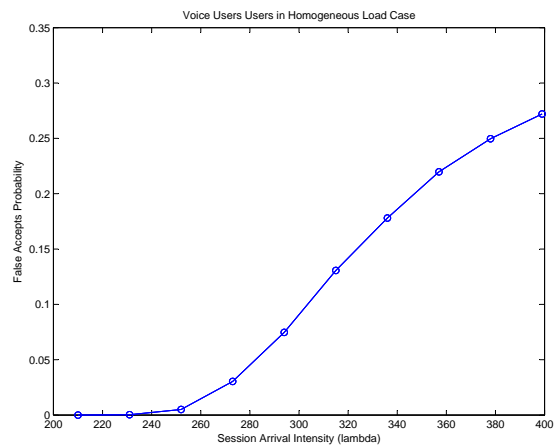
(f) False Accepts Probability

Figure 7.1: Homogeneous Load Case for Voice Users
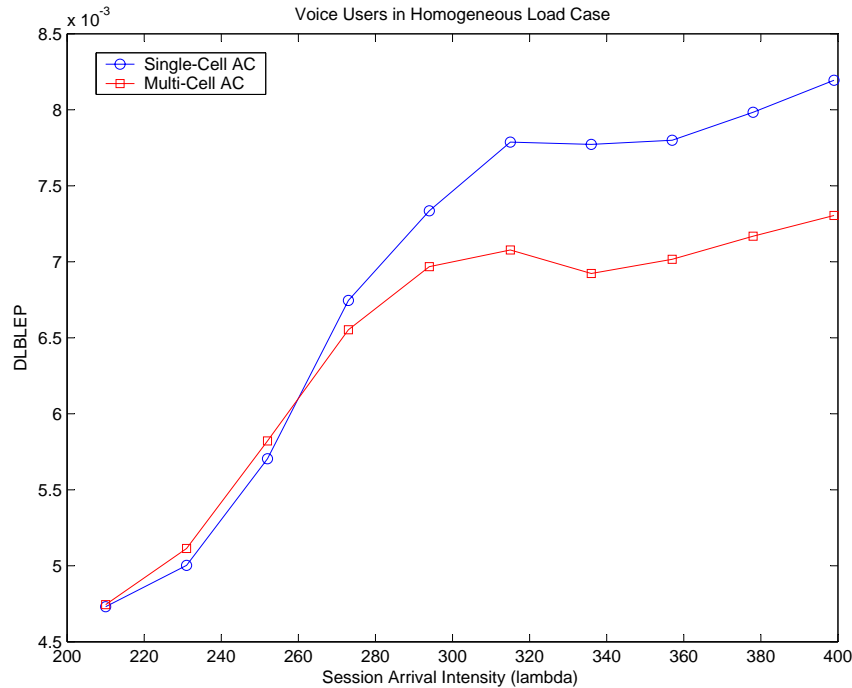
Figure 7.2: Downlink Block Error Probability

Both uplink and downlink block error probabilities show differences between Multi-Cell and Single-Cell admission controls, see Figures 7.6(a), 7.6(b), 7.6(d), and 7.6(f). This especially true when the block error probabilitiy is plotted as a function of the averange number of users in the system. The gains range from 0 to 7.5% with the Multi-Cell admission control.

As observed in the hotspot case, in order to avoid false accepts that could decrease the quality of service for users admitted in the central cell, e.g. the outage probability, a slight change in the η_{th} would be necessary, around 0.55 as it can be seen in Figure 7.7, which also represents waste of capacity for the Single-cell admission control.

7.2   Video Users

The second set of simulations examined the case for the video users. It followed a similar approach as considered for the voice users. The important characteristics that distinguish video and voice users are their peak bitrates, 12.2kbps for voice and 64kbps for video, and the fact that video users are modeled without downlink traffic, in order to eliminate outages due to downlink issues. Again, the primary goal for these simulations was to show a performance comparison between Single-cell and Multi-cell Admission Control Algorithms for different traffic models. Table 7.2 summarizes the specific simulation parameters.

7.2.1   Homogeneous Load Case

Comparing results obtained from voice and video users in the Homogeneous load case, blocking probabilities are similar in Figures 7.8(a) and 7.1(a). False accepts probability (Figure 7.8(d)) indicates a slight difference between both admission control algorithm results regarding the uplink block error probability (Figure 7.8(b)). The same result occurs for users currently served by the system (see Figure 7.8(c)). Dropping probabilities have very low values, due to the absence of downlink traffic. In despite of that, a substantial lower outage probability can be seen in favor of the Multi-Cell admission control (see Figures 7.8(c) and 7.8(d)).
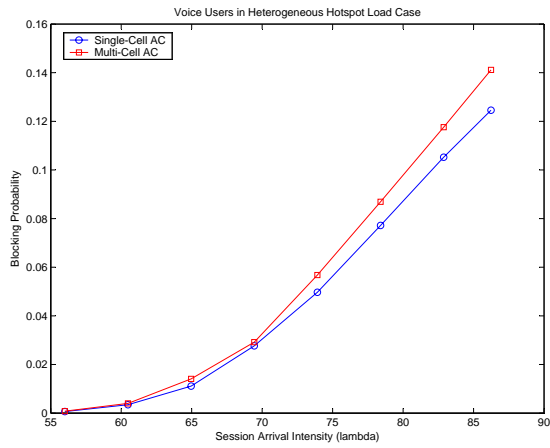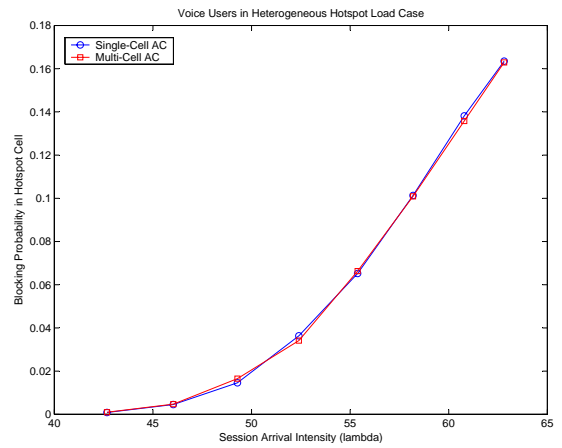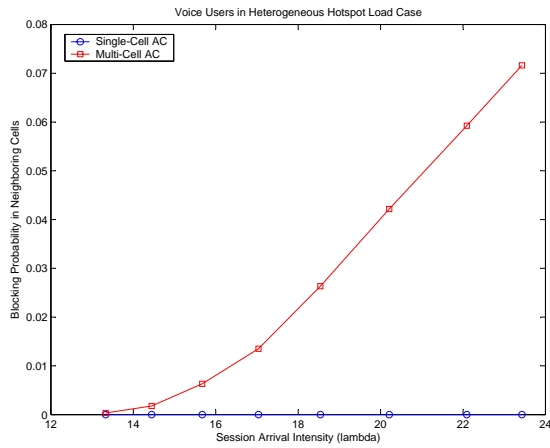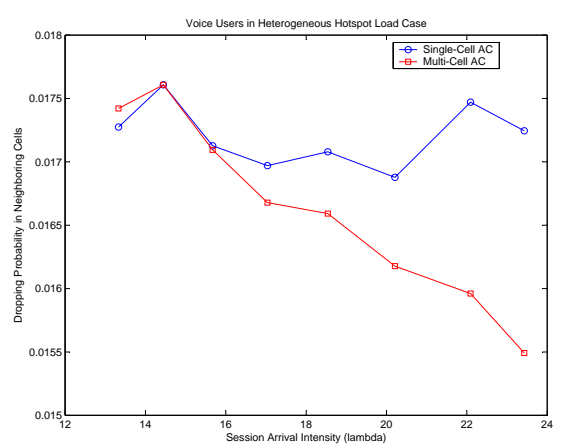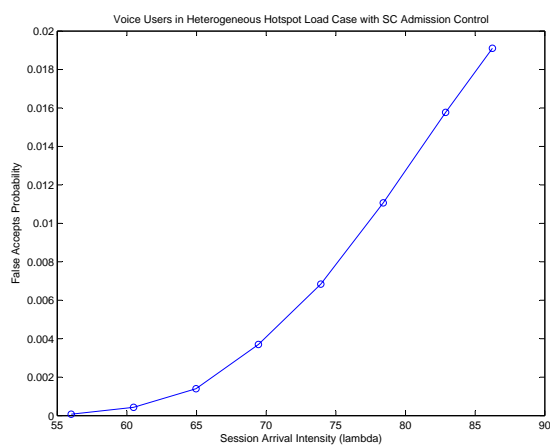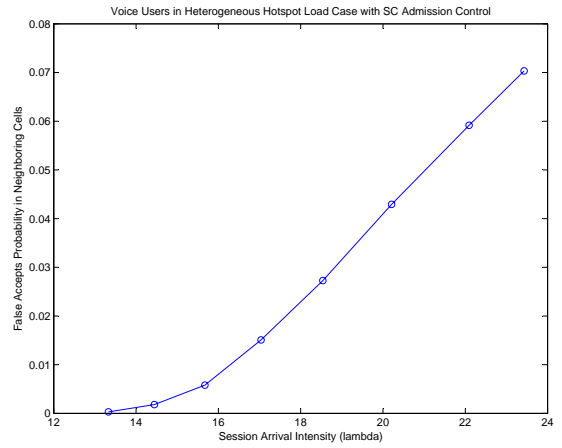
Figure 7.3: Heterogeneous Hotspot Load Case for Voice Users
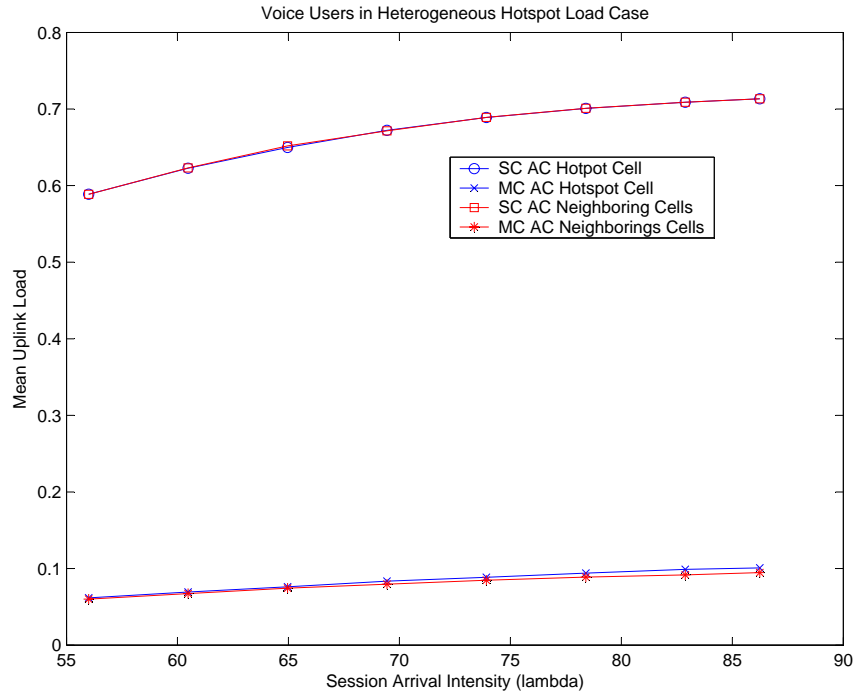
Figure 7.4: Uplink Load for Hotspotted and Neighboring Cells

Admission Control	Users	Load Case	η_{th}	$\lambda_{initial}$ ++ increment
SC	Video	Homogeneous	0.75	42++10%
MC	Video	Homogeneous	0.75	42++10%
SC	Video	Hotspot	0.75	10.5++5%
MC	Video	Hotspot	0.75	10.5++5%
SC	Video	"Hotround"	0.75	42++10%
MC	Video	"Hotround"	0.75	42++10%

Table 7.2: Simulation Parameters for Video Users

7.2.2   Heterogeneous Hotspot Load Case

Results observed in Figure 7.9 allowed us to make similar analysis to the Voice users in the Heterogeneous Hotspot load case. As expected, very little difference between the Single and Multi-Cell is observed in the hotspot cell (Figure 7.9(b)), while Figures 7.9(c) and 7.9(f) point to the actual difference that contributes to a slightly more conservative admission control taken with the Multi-Cell algorithm. Similarly to the hotspot load case with voice users, the weight factor was set to 1, which naturally resulted in very close blocking probabilities observed in the hotspot cell (Figure 7.9(b)).

No significant change is noticed in Figure 7.9(d) due to the not expressive overall false accepts probability shown in Figure 7.9(e).
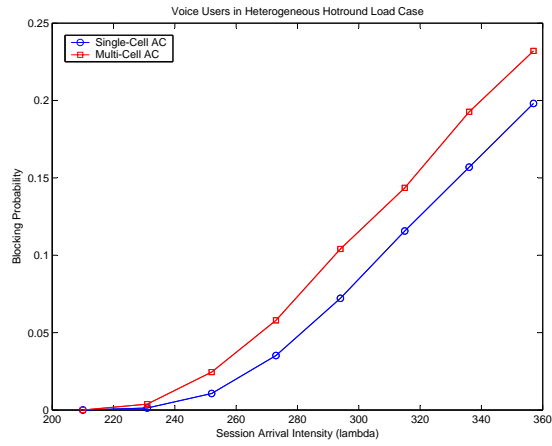
(a) Overall Blocking Probabilitiy
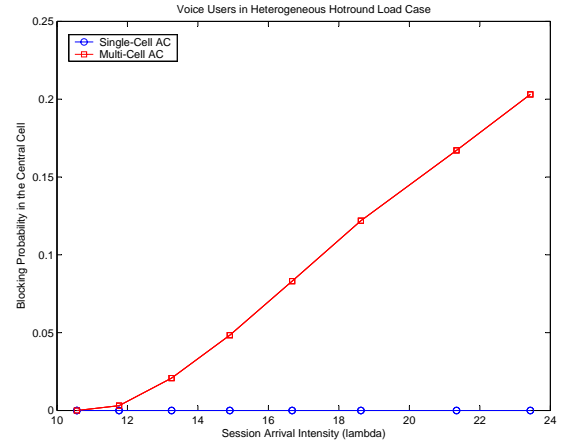
(b) Central Cell Blocking Probability
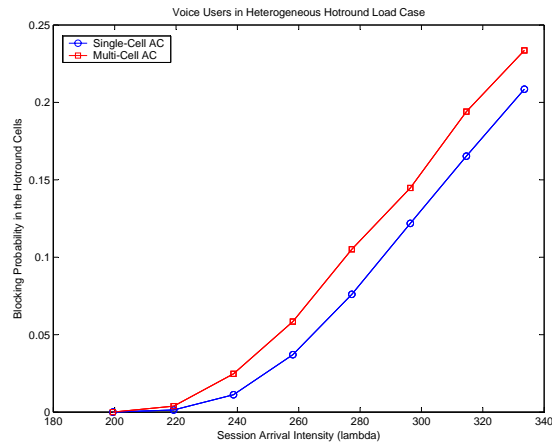
(c) Hotround Cells Blocking Probability
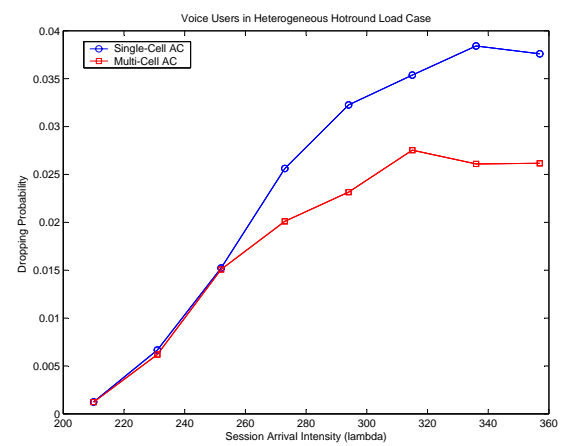
(d) Overall Dropping Probability
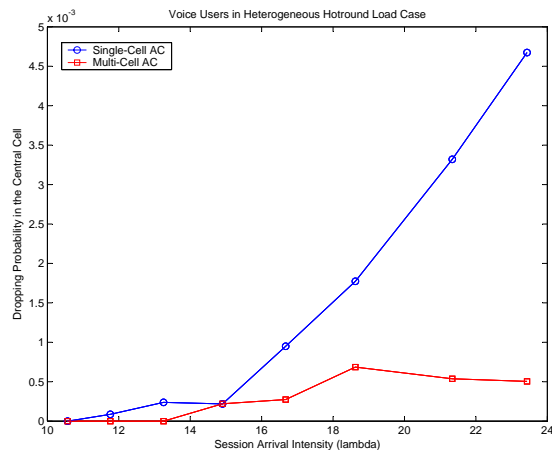
(e) Central Cell Dropping Probability
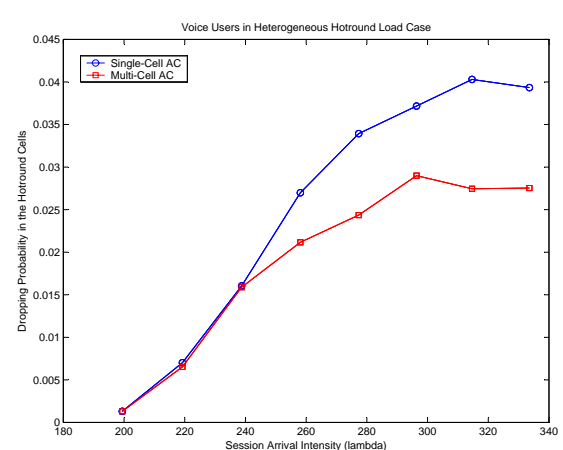
(f) Hotround Cells Dropping Probability

Figure 7.5: Heterogeneous Hotround Load Case for Voice Users
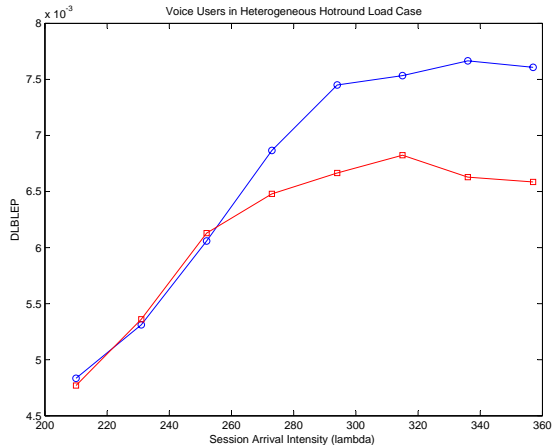
(a) DLBLEP
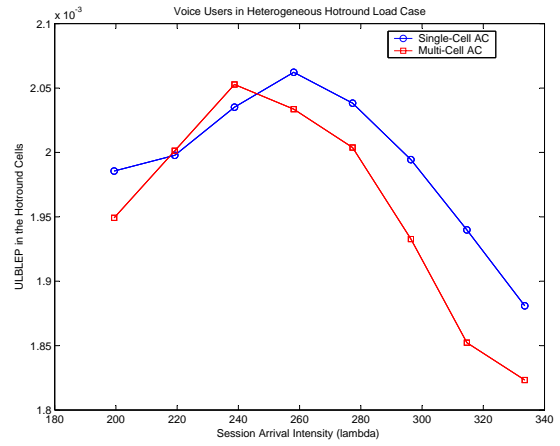
(b) ULBLEP Hotround Cells
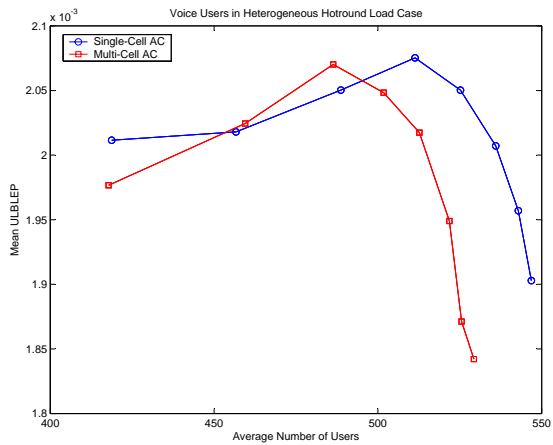
(c) ULBLEP - f(users)
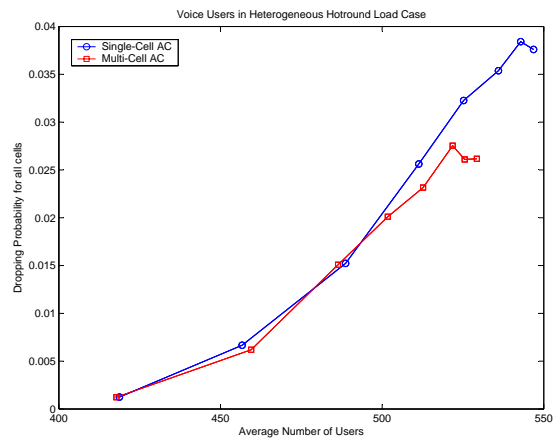
(d) Dropping Probability - f(users)
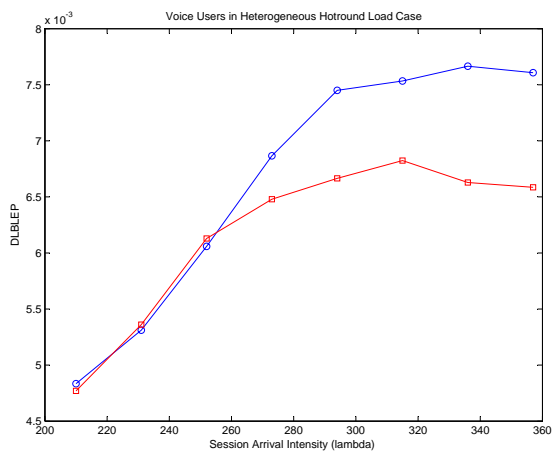
(e) Downlink Block Error Probability
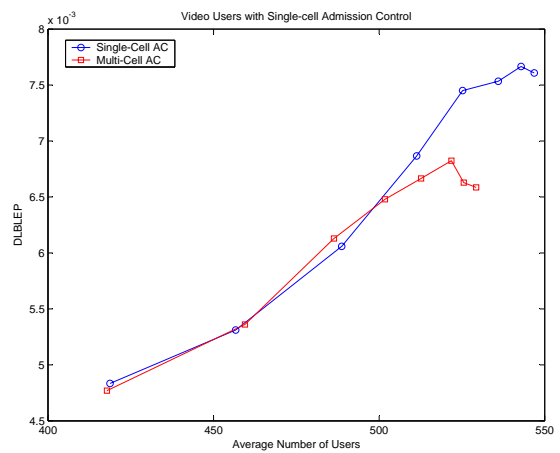
(f) DLBLEP - f(users)

Figure 7.6: Heterogeneous Hotround Load Case for Voice Users
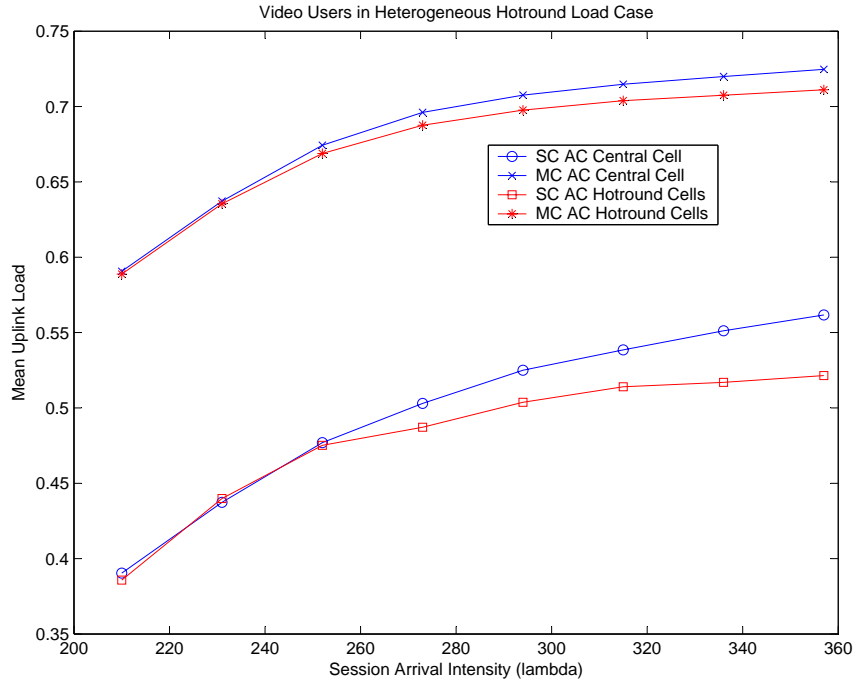
Figure 7.7: Uplink Load for Central and Hotround Cells

Similarly to the Voice users in the hotspot load case, in order to avoid the false accepts probability in the neighboring cells, the Single-Cell admission control η_{th} should be decreased from 0.75 to some value around 0.20 in all the six neighboring cells, implying a significant loss of capacity (see Figure 7.10).

7.2.3 Heterogeneous Hotround Load Case

In the Heterogeneous Hotround load case, results were similar to the ones from the Homogenous case with Video users. Although an increasing difference can be noticed between blocking probabilities from Single and Multi-Cell admission control since the first plotted point, i.e. $\lambda = 36(persecond)$ (see Figures 7.11(a) and 7.11(b)), Multi-Cell contribution regarding uplink block error probability becomes more significant starting from $\lambda = 47(persecond)$.

Figure 7.12 shows the mean uplink load for hotround and central cells. In order to avoid false accepts with the Single-Cell admission control in the central cell, decreasing η_{th} to around 0.50 in the central cell should be considered, reflecting in a loss of capacity.

7.3 UL128(Kbps) Users

The third and last set of simulations regarding the UL128 Users aimed to consider both rigid and elastic traffic models with the Admission Control algorithms. UL128 Users are defined as having 128kbps peak bit rate, and minimum guaranteed bit rate, 16kbps, 32kbps, 64kbps, and 128kbps for respective maximum slowdown rate $\hat{a}=8$, $\hat{a}=4$, $\hat{a}=2$, and $\hat{a}=1$. The reader can refer to Sections 4.6.2, 4.6.3, and 4.6.4 which explain in detail the slowdown mechanisms. The legends of the graphics in the next few pages refer to SC as the Uncoordinated Slowdown, MC as the Coordinated Unfair Slowdown Mechanism, and MCF as the Coordinated Fair case. The same applies to results comments. Table 7.3 summarizes the specific simulation parameters. MCF and MC were submitted to the same set of inputs.
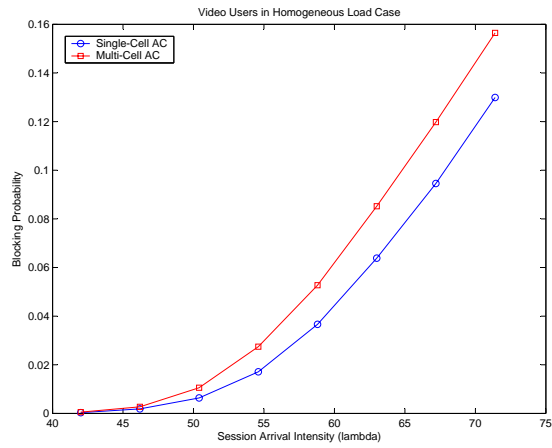
(a) Overall Blocking Probabilitiy
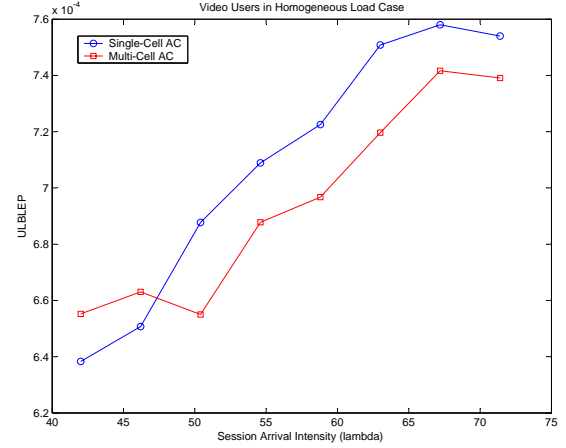
(b) Overall Block Error Probability
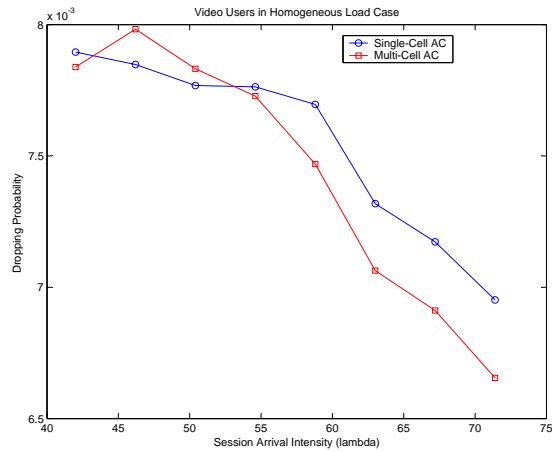
(c) Dropping Probability
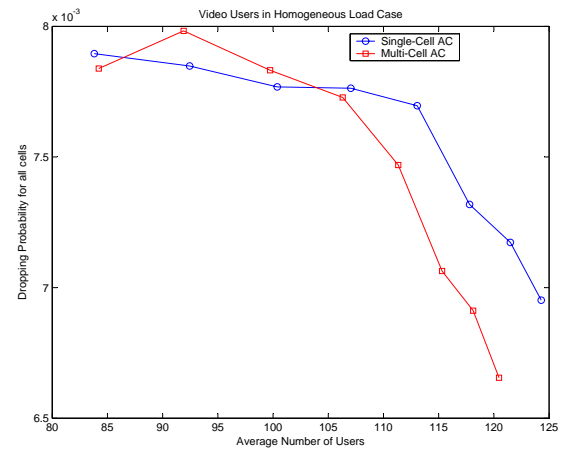
(d) Dropping Probability - f(users)
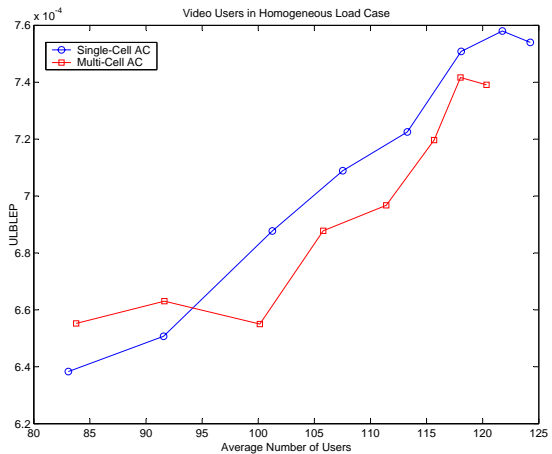
(e) Block Error Probability - f(users)
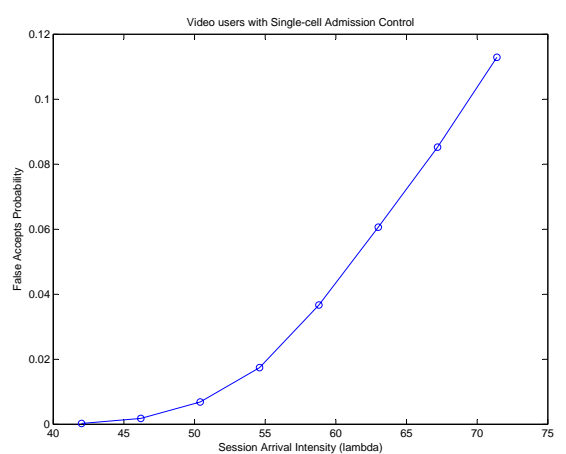
(f) Overall False Accepts Probability

Figure 7.8: Homogeneous Load Case for Video Users
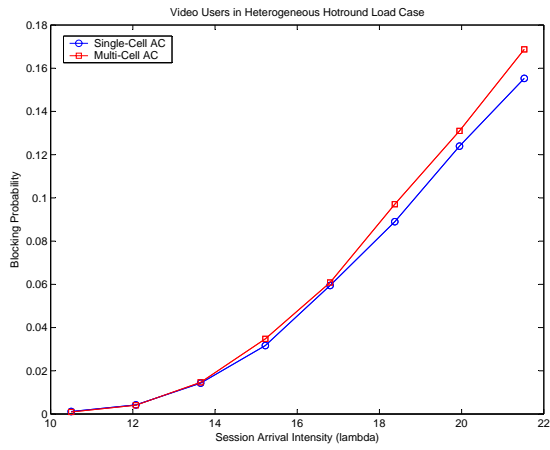
(a) Overall Blocking Probabilitiy
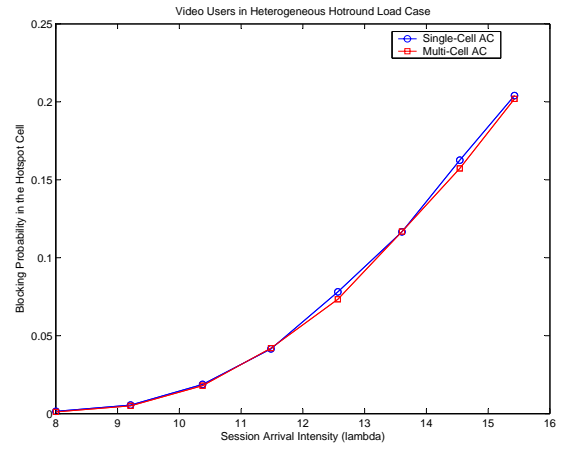
(b) Hotspot Cell Blocking Probability
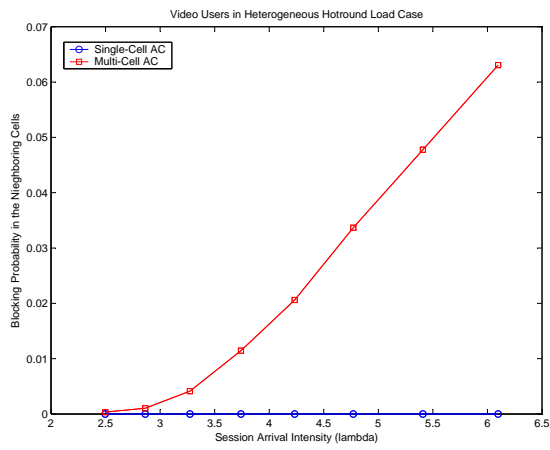
(c) Neighboring Cells Blocking Probability
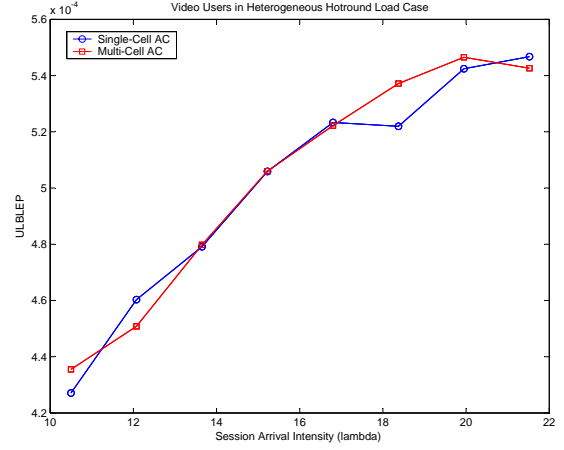
(d) Overall Block Error Probability
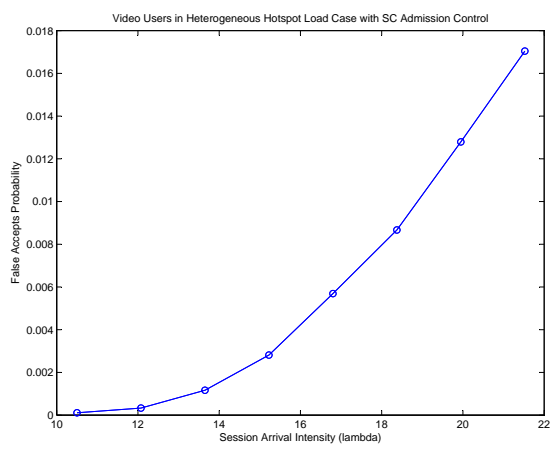
(e) Overall False Accepts Probability
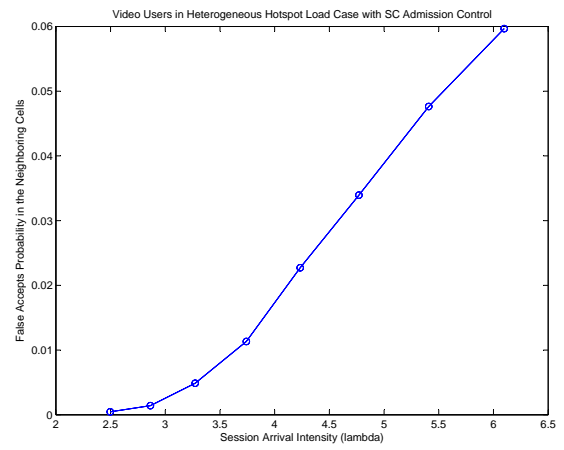
(f) Neighboring Cells False Accepts Probability

Figure 7.9: Heterogeneous Hotspot Load Case for Video Users
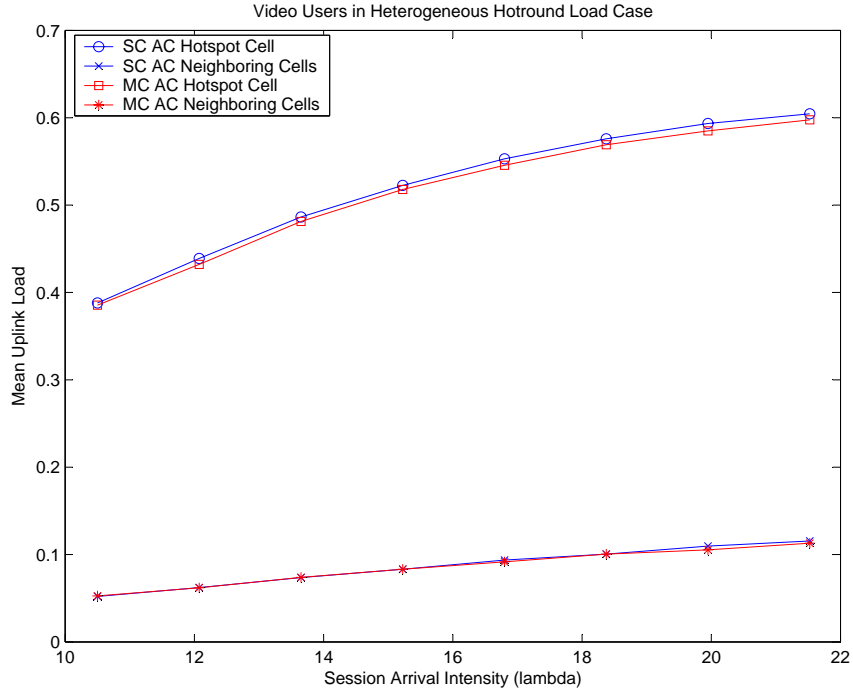
Figure 7.10: Uplink Load for Hotspot and Neighboring Cells

Admission Control	Users	Load Case	â	η_{tg}	η_{th}	$\lambda_{initial}$ ++ increment
SC	UL128k	Homogeneous	-	-	0.75	14.875++10%
SC	UL128k	Homogeneous	1	0.75	0.85	14.875++10%
SC	UL128k	Homogeneous	2	0.75	0.85	14.875++10%
SC	UL128k	Homogeneous	4	0.75	0.85	14.875++10%
SC	UL128k	Homogeneous	8	0.75	0.85	14.875++10%
MC	UL128k	Homogeneous	-	-	0.75	14.875++10%
MC	UL128k	Homogeneous	1	0.75	0.85	14.875++10%
MC	UL128k	Homogeneous	2	0.75	0.85	14.875++10%
MC	UL128k	Homogeneous	4	0.75	0.85	14.875++10%
MC	UL128k	Homogeneous	8	0.75	0.85	14.875++10%

Table 7.3: Simulation Parameters for UL128(kbps) Users

Uncoordinated vs Coordinated Unfair Results

Analyzing blocking probabilities in Figure 7.14 we can notice a significant impact of the slowdown mechanisms on both Single and Multi-Cell admission controls. Increasing maximum slowdown rates ($\hat{a} = 2, 4$, and 8) in the Single-Cell case has showed less admitted calls, however, still accepting more
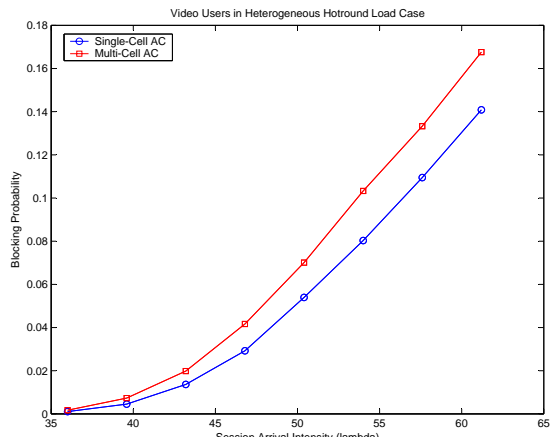
(a) Overall Blocking Probabilitiy
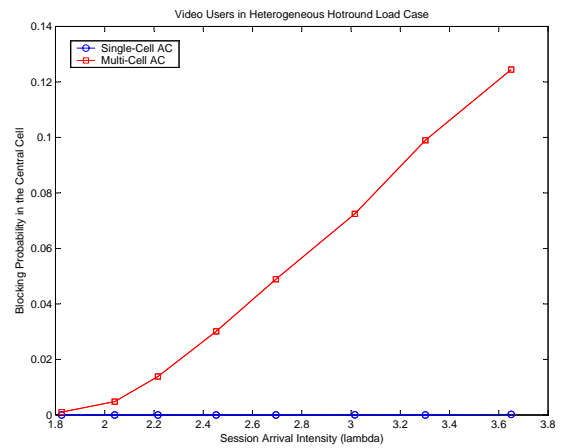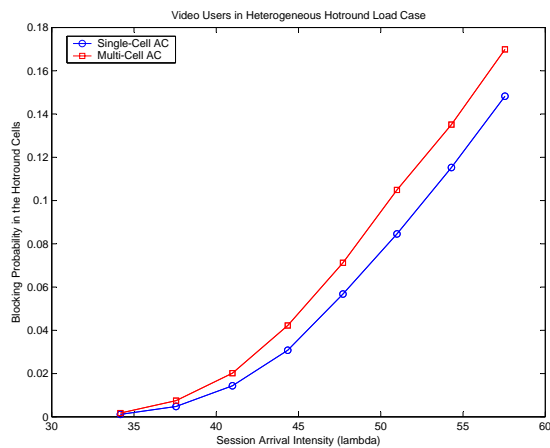
(b) Central Cell Blocking Probability

(c) Hotround Cells Blocking Probability
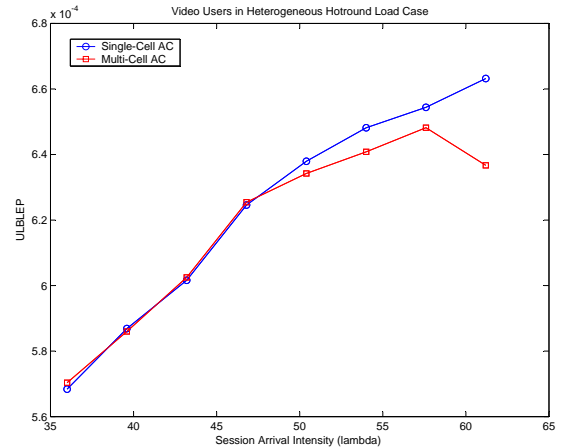
(d) Overall Block Error Probability
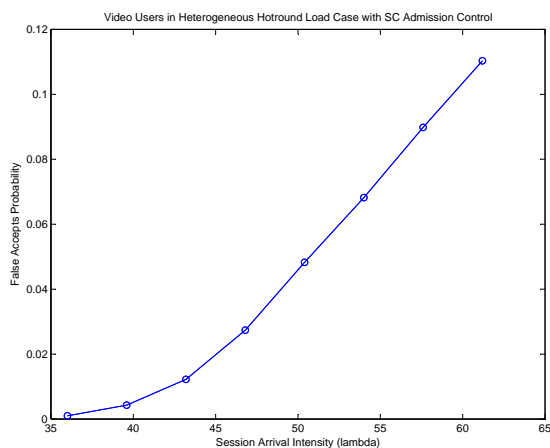
(e) Overall False Accepts Probability
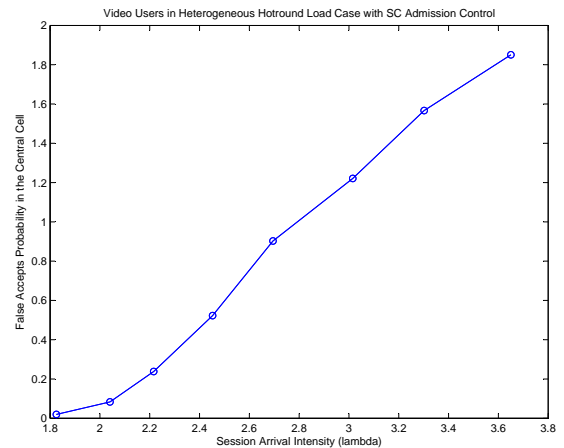
(f) Central Cell False Accepts Probability

Figure 7.11: Heterogeneous Hotround Load Case for Video Users
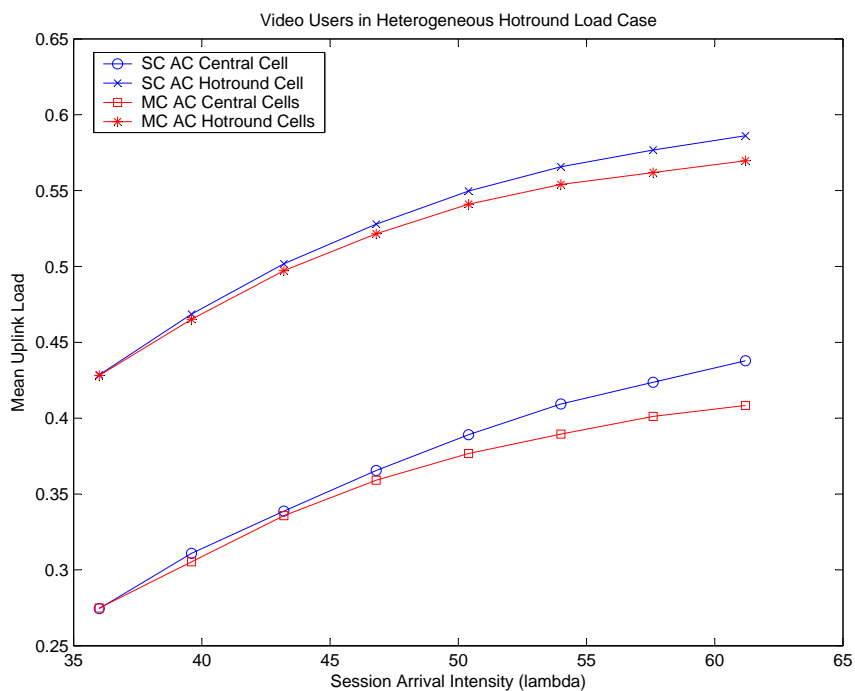
Figure 7.12: Uplink Load for Hotround and Central Cells
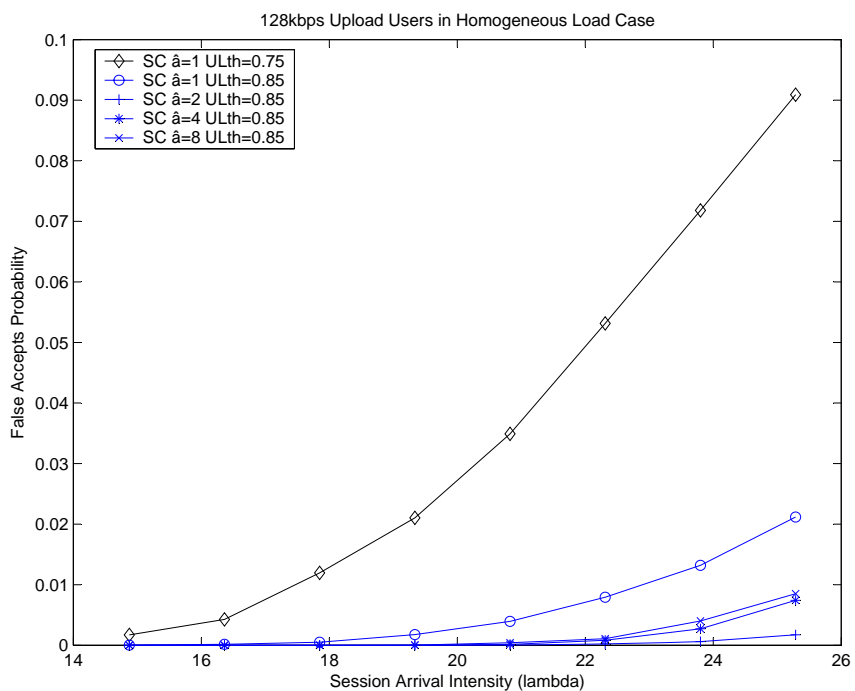
Figure 7.13: False Accepts Probability

users than the case with only "UL128 $\hat{a} = 1$" users. Contrarily, the Multi-cell Coordinated Unfair slowdown indicated similar blocking probabilities until $\lambda = 23.8(persecond)$. From this point on, the

(a) Blocking Probabilities

(b) Zoomed
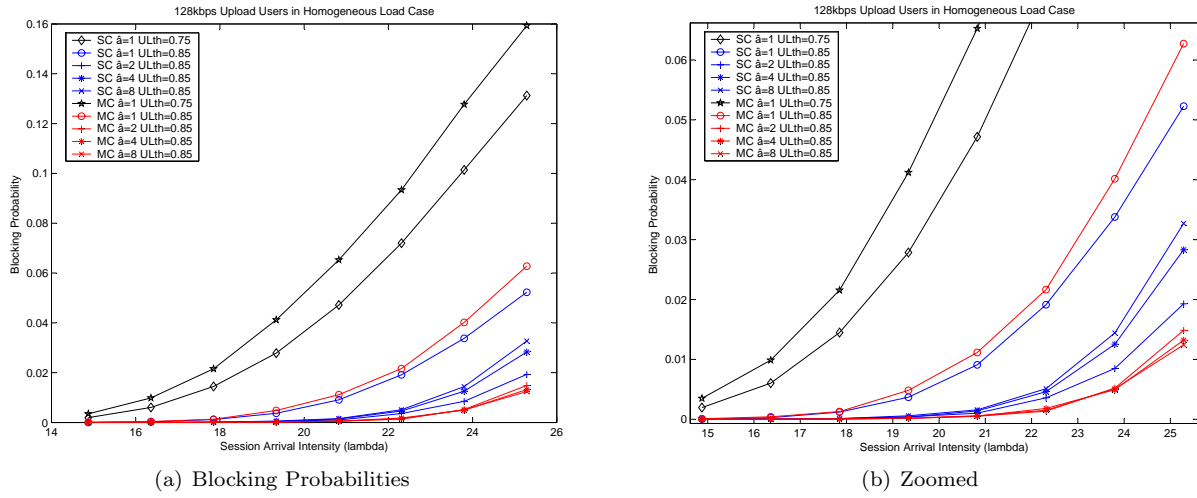
Figure 7.14: Blocking Probabilities for UL128 users

efficient use of the larger state space with $\hat{a} = 8$ starts to give place to larger number of slowdowns, which allows more users to be admitted into the system. In brief, the Multi-Cell Coordinated Unfair slowdown succeeded to decrease the blocking probability in approximately 5%, while the Single-Cell Uncoordinated case succeeded between 2% and 3.2% ($\hat{a} = 8$ and 2 respectively). This different behavior is due to the occurrence of false slowdowns that happen in the Single-Cell Uncoordinated case, which increases with larger $\hat{a}$'s.
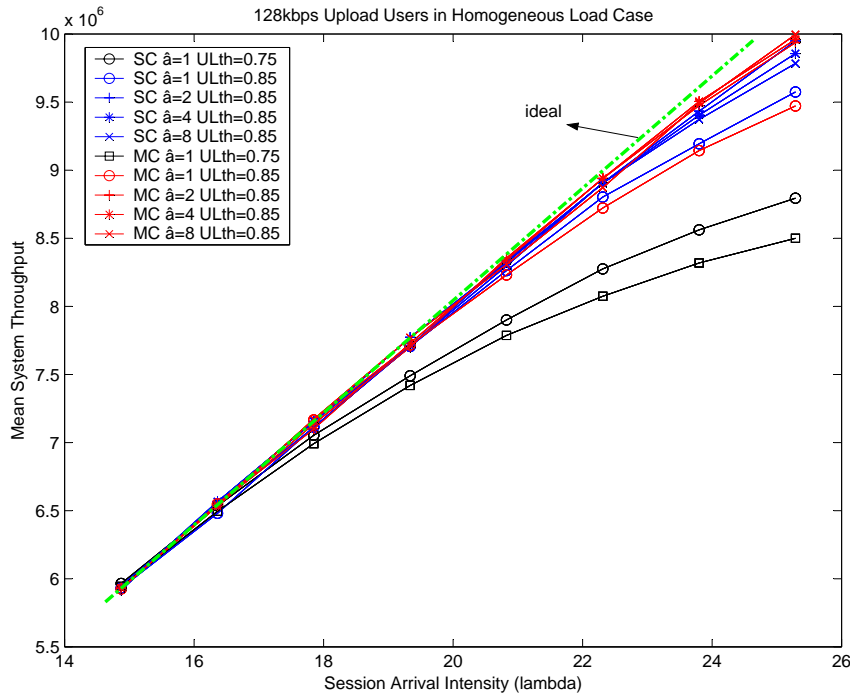
Figure 7.15: Mean System Throughput for UL128 users

Analyzing Figure 7.15 one can easily see a significant better performance for both SC and MC slowdown mechanisms, when compared to $\hat{a}=1$ cases. Tracing an ideal line that represents the case when all users can be slowed down indefinitely, with perfect power control, and thus leaving room to the system accept infinite calls. All three MC with slowdown cases have presented themselves closer to this ideally defined line.

(a) ULBLEP vs Session Arrival Intensity

(b) ULBLEP vs Mean UL Load
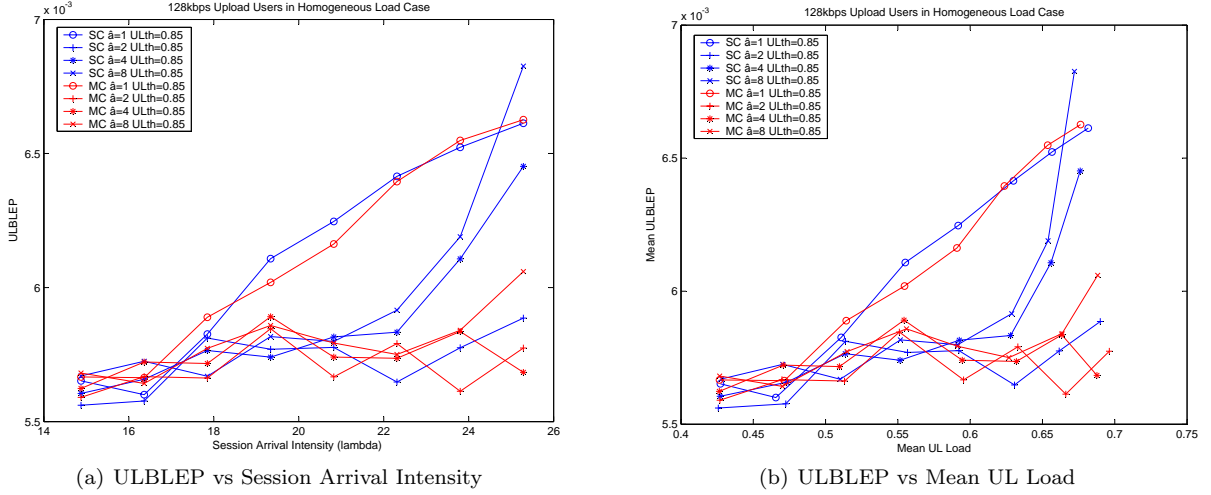
Figure 7.16: Uplink Block Error Probability for UL128 users

Basing on ULBLEP Figures 7.16(a) and 7.16(b), no significant different is noticed between Single and Multi-Cell admission control when $\hat{a} = 1$. This result is due from the presence of a function in the simulator that changes the Transport Format Combination (TFC) according to radio quality statistics (e.g. ULBLEP) taken from the users. Even though, no expressive difference is observed between these two cases, the influence of false slowdowns is interestingly noticed with SC $\hat{a} = 4$ and 8, yielding an increase of approximately 10% and 18% in the uplink block error probability for $\lambda = 25.4(persecond)$, respectively. Interestingly, SC $\hat{a} = 2$ succeeds to maintain similar ULBLEP when compared to any of the three MC Coordinated Unfair slowdown cases.

Figure 7.17 illustrates the overall mean user throughput. It is interesting to notice a decrease in the user throughput of 10%, 12%, and 14% ($\lambda = 25.4(persecond)$) for $\hat{a}=8$, $\hat{a}=4$, and $\hat{a}=2$, respectively with MC slowdown. This behavior comes from the fact that when users are slowed down in a cell that has exceeded the η_{tg}, having larger $\hat{a}$'s is counted as an advantage because the slowdown process can exploit a larger system state space by choosing "more convenient slowable" users, thus decreasing the total number of slowed blocks. The SC cases presented higher mean throughputs for users with $\hat{a}=4$ and 8. Due to more frequent false slowdowns in such cases, much frequent noise rise violations take place (see Figure 7.18(b)) which results in users frequently and erroneously with higher bit rates than the minimum guaranteed bit rate.

Figures 7.18, 7.19, and 7.20 serve as foundations in order to sustain the previous graphics and conclusions (considered for $\lambda = 25.4(persecond)$). In brief words Figure 7.18 intends to show the influence of false slowdowns in the overall probability of noise rise violations, while Figure 7.19 indicates a better interference equalization around ηtg for higher $\hat{a}$'s.

Uncoordinated vs Coordinated Fair Results

Considering Figures 7.21(a), one can clearly see that the MCF has achieved lower blocking probabilities than the SC case. However, interestingly MCF $\hat{a}=2$ has shown increased blocking probability for $\lambda=23.8(persecond)$ and specially for $\lambda=25.4(persecond)$. This is justified by the fact that MCF $\hat{a}=2$ cannot handle anymore slowdowns in the system, thus setting all users to the minimum bit rate in highly

(a) Mean User Throughput

(b) Zoomed
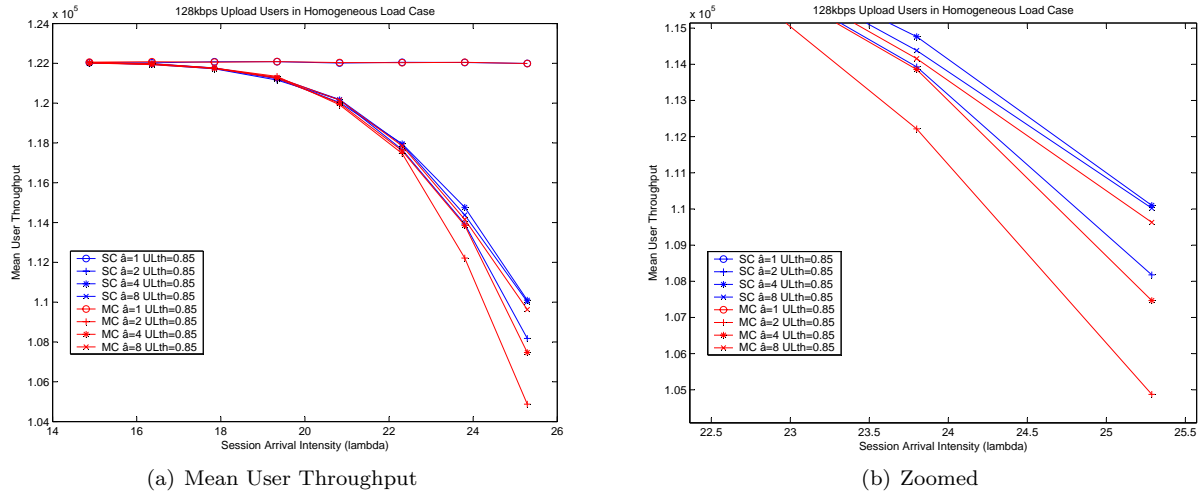
Figure 7.17: Mean User Throughput for UL128 users

(a) Overall CDF for $\lambda = 25.4(per\,second)$

(b) Zoomed
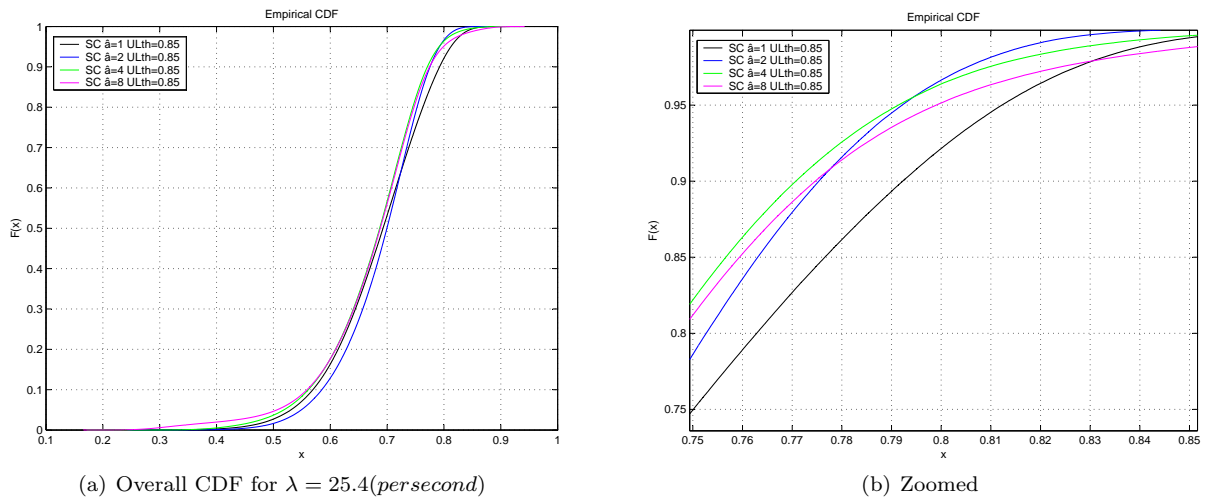
Figure 7.18: Uplink Load Cumulative Distribution Function for Uncoordinated Slowdown

(a) Overall CDF for $\lambda = 25.4(persecond)$
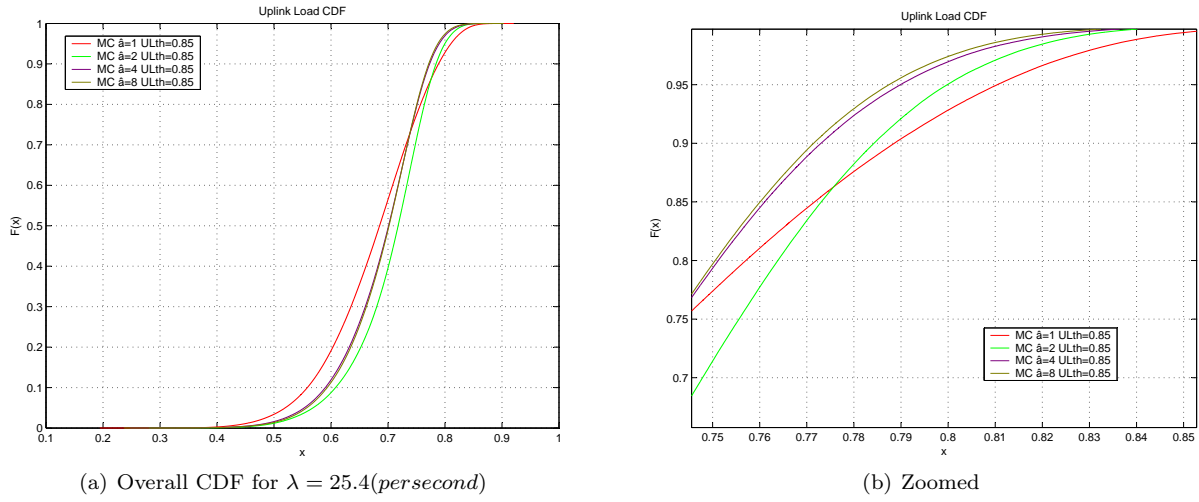
(b) Zoomed

Figure 7.19: Uplink Load Cumulative Distribution Function for Coordinated Unfair Slowdown

(a) Overall CDF for $\lambda = 25.4(persecond)$
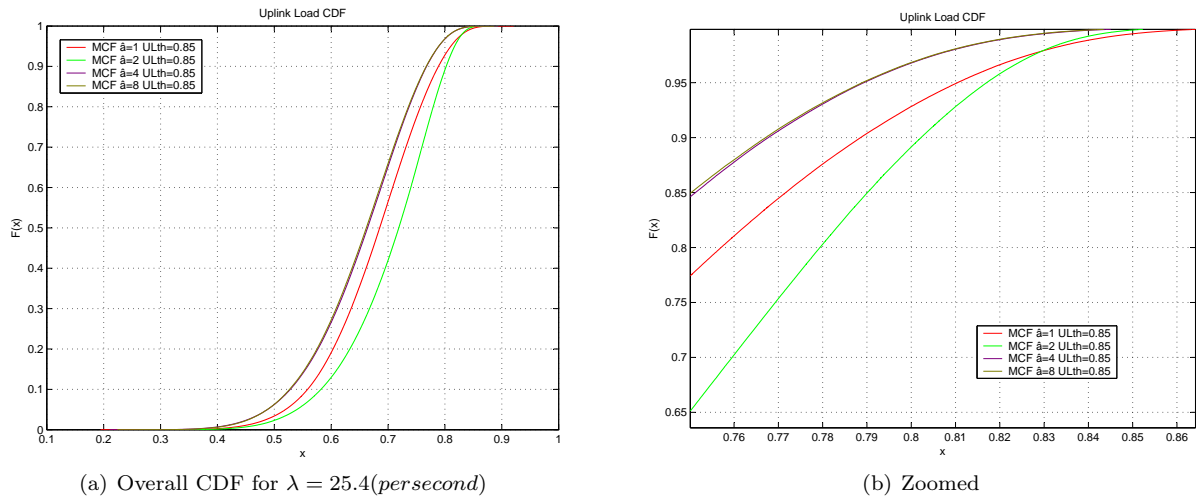
(b) Zoomed

Figure 7.20: Uplink Load Cumulative Distribution Function for Coordinated Fair Slowdown
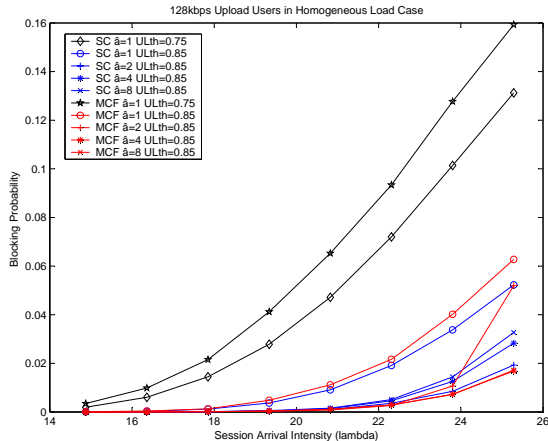
(a) Blocking Probabilitiy
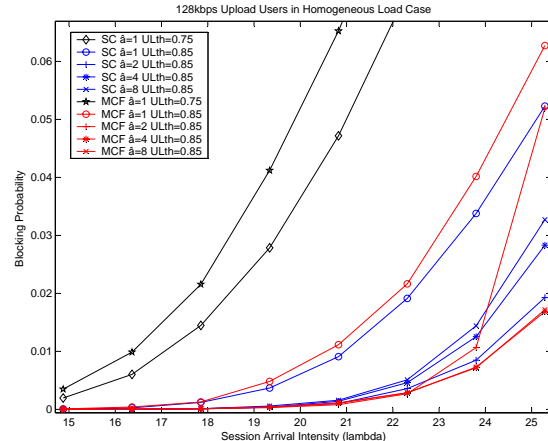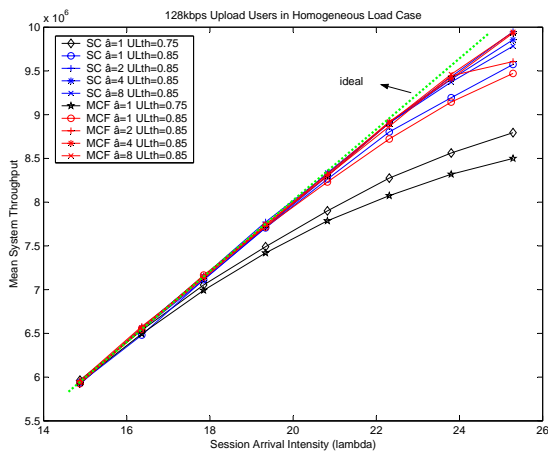
(b) Zoomed

(c) Mean System Throughput
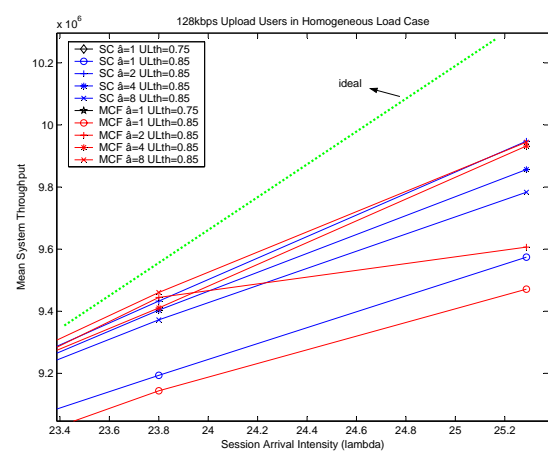
(d) Zoomed
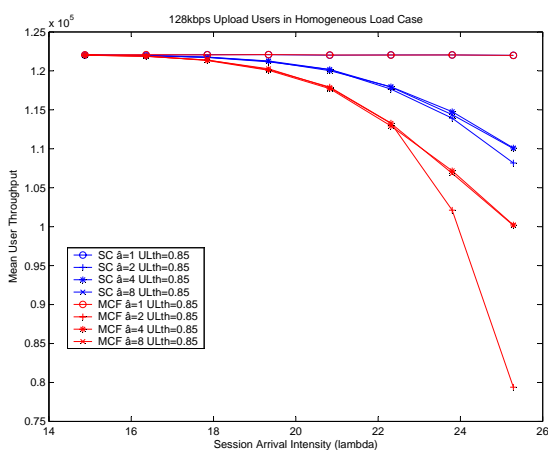
(e) Mean User Throughput
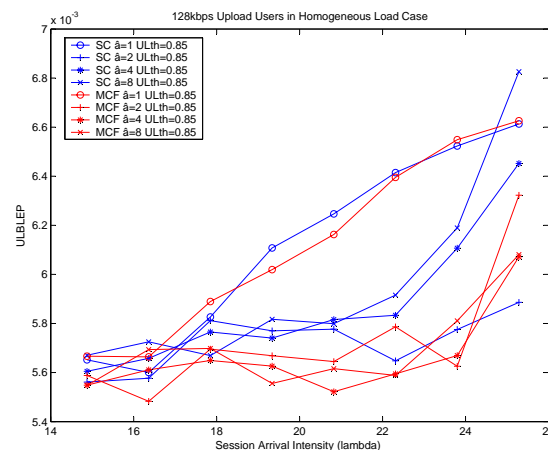
(f) Uplink Block Error Probability

Figure 7.21: Uncoordinated vs Coordinated Fair Results

loaded situations, affecting the overall mean user throughput (see Figure 7.21(e)). Figure 7.3 shows this increase of users with 4 blocks. Similar behavior can be suggested with MCF $\hat{a}$=4 for higher λ's, and further with MCF $\hat{a}$=8.

Regarding the uplink block error probability, a slight increase can be noticed for all cases for the last two plotted points of each line, with the exception of SC $\hat{a}$=2.

The most important conclusion from this set of graphics is that MCF is able keep low noise rise levels and increase the overall system capacity for a limited session arrival intensity, at the expense of a decrease in the mean user throughput. When comparing the Coordinated Fair (MCF) and Unfair (MC) cases, wee that the later is done more coherently, yielding higher user and system throughputs, and still keeping low the blocking probabilities.

The better performance presented by the Coordinated Unfair case has the drawback related to computational issues. Just for illustration matters, consider a 7-cell-system with 70 users in a given instant. By allowing users to occupy any of the 8 blocks states (1, 2, 3, 4, 5, 6, 7, or 8 given transport blocks), from the combination theory, the total system state space becomes $\binom{70}{8} = 9.4404e+009$ different states. Otherwise, by allowing only users to occupy at most 2 transport block states (X and $X - 1 \parallel 1 < X \leq$) the system state space becomes much narrower with $70 \cdot 69 \cdot 7 = 33810$ different states for each MCF slowdown process.

7.4   Summary

Through all plotted results and driven conclusions, it has been cleared the important contribution from multi-cell based RRM algorithms. Considering all the scenarios, with voice, video, and UL128 users, modeled as rigid and elastic traffic, results have shown that the higher conservativeness employed by Multi-cell based algorithms indicates a coherent better overall performance.

Specially results from the Section 7.3 regarding Admission Control combined with slowdown techniques have shown that load and user information concerning every cell is fundamental in order to increase both system capacity (from blocking probability) and improve user's experienced quality of service (dropping and ULBLEP).
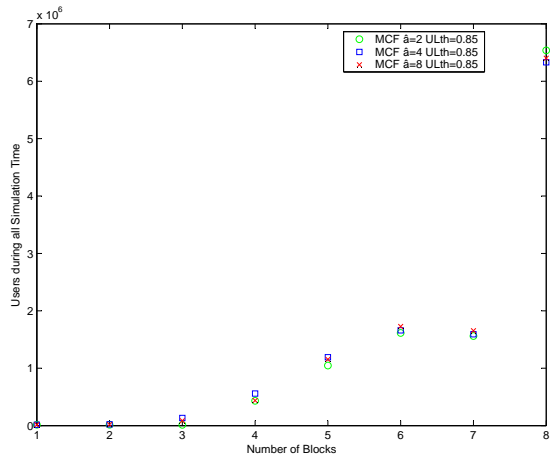
(a) Number of Blocks per User λ=22.3($persecond$)
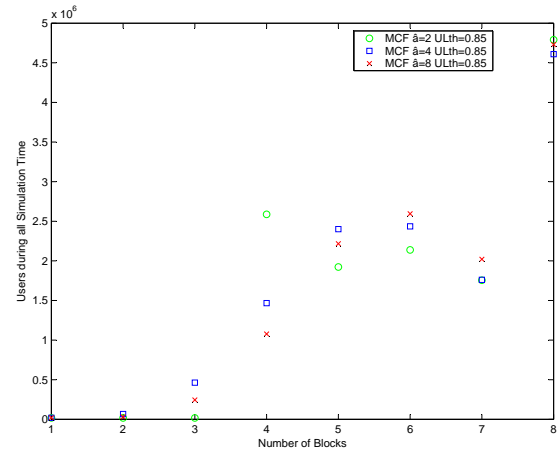
(b) Number of Blocks per User λ=23.8($persecond$)
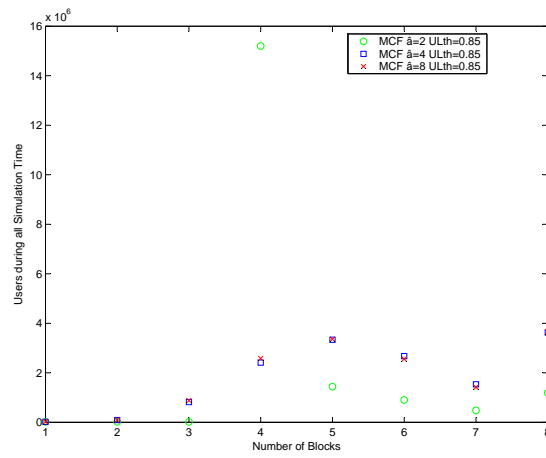
(c) Number of Blocks per User λ=25.4($persecond$)

Figure 7.22: Number of Blocks Distribution

This page intentionally contains only this sentence.

Chapter 8

Conclusions

A WCDMA system, just as any other communication network, has limited resources, meaning that a limited amount of bits are allowed to be transmitted based upon radio interface constraints. By analyzing and exploiting such radio issues, operators and manufacturers have additional opportunities to improve their systems and networks in order to maximize the user's experienced Grade of Service (GoS) and Quality of Service (QoS).

In this thesis capacity enhancing techniques have been investigated for the Uplink of WCDMA, regarding Multi-Cell admission control associated with rate control mechanisms.

The thesis has evaluated system level performance and the achievable capacity gains of these techniques. Furthermore, the required radio resource management (RRM) algorithms to deploy these different load control functions has been considered. This research relies on extensive simulations, considering several different scenarios and algorithms as inputs. Theoretical analyses have been carried out in order to validate the results obtained with the simulations and to provide an easier way to assess the influence of various factors in the overall system performance.

In summary, the benefits of Multi-Cell over Single-Cell Admission Control over both rigid and elastic traffic are increased system capacity and overall provisioned Quality of Service (QoS). Furthermore, it has been shown that the "coupling factor" is an essential foundation for Multi-Cell algorithms in interference share environments. Such a principle has been further adapted to rate control mechanisms, which permitted more refined multi-cell RRM, leading to improve both system capacity and QoS.

These results indicated very important contributions for research in WCDMA networks, which faces constantly evolving demands for new and advanced services. In order to face other competing radio access technologies, WCDMA multi-cell RRM techniques come as an important addition in order to efficiently exploit all the potential inherent to this technology.

This page intentionally contains only this sentence.

Chapter 9

Future Work

As described in Chapter 4 the slowdown implemented algorithms did not consider SIR and user position when choosing one user to be slowed down. Rather, in the Coordinated Unfair case, a random user belonging to the current "fastest" group of users, and served by the highest loaded cell was chosen and slowed down. If the highest loaded cell did not have any "slowable" users, the second highest loaded cell was chosen, and so forth.

One should indicate that this slowdown mechanism could be improved, by considering user specific data, such as SIR, user position, other fairness principles, priority, etc. The scope of this thesis work has not included describing such a complex rate control model, but evaluating how elastic sessions could impact the studied Admission Control mechanisms, particularly in Single-Cell and Multi-Cell based algorithms.

These results were based on a Poisson arrival process and exponentially distributed data creation. Due to increasing differences in the nature of user traffic, other arrival and data creation processes should be considered in order to reach more specific conclusions in multi-cell RRM, especially regarding admission and rate control.

The conclusions reflected the performance advantages of multi-cell based load control functions in a steady-state-simulation. Further research should be done concerning "heavy-tailed" false accepted users, i.e. with huge amounts of data to transmit, and how they affected some calls in particular, and the entire system. Such a scenario represents what is denoted as "transient" situations.

Furthermore, the present work has focused mainly on Admission Control (AC) and other Load Control (LC) functions, i.e. dropping and slowdown. According to [20], interworking of AC and LC functions can be further combined with the Packet Scheduling (PS) function. Figure 9.1 illustrates such an interaction, following the same Noise Rise vs. Load principle previously approached in Chapter 4. The advantage from the use of the coupling factors could be employed by PS algorithms, as well as PS information used by AC and LC functions, in order to increase system capacity and user's experienced QoS.
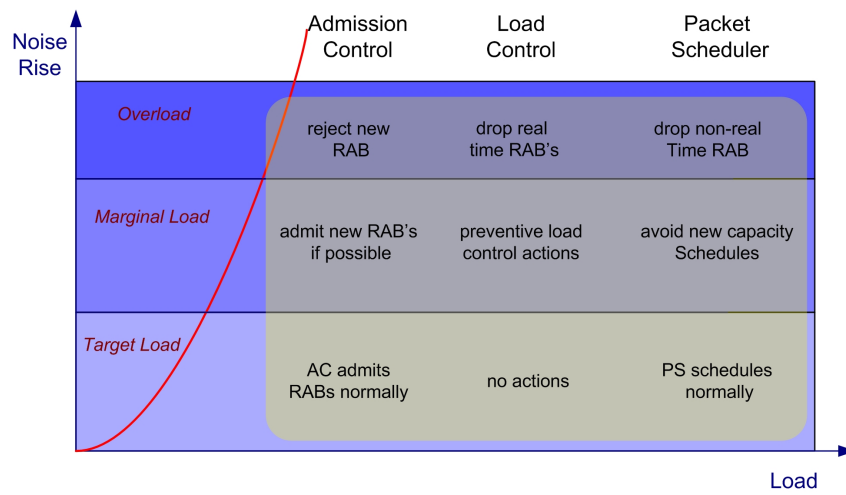
Figure 9.1: Interworking Actions of AC, PS, and LC Functions [20]

Chapter 10

Appendix

Below follows the confidence intervals for each figure presented in Chapter 7.

We define as x the 95 percentile confidence interval divided by the mean value. Different confidence intervals for each point in each figure diverge because the higher session arrival intensity, the more often events occur.

Figure	Percentile Confidence Variation (x) over Mean Value
Figure 7.1 (a)	0.01% < x < 0.05%
Figure 7.1 (b)	0.03% < x < 0.10%
Figure 7.1 (c)	0.03% < x < 0.10%
Figure 7.1 (d)	6.5% < x < 6.8%
Figure 7.1 (e)	6.5% < x < 6.8%
Figure 7.1 (f)	0.1% < x < 0.5%
Figure 7.2	3.5% < x < 3.8%
Figure 7.3 (a)	0.01% < x < 0.04%
Figure 7.3 (b)	0.01% < x < 0.04%
Figure 7.3 (c)	0.01% < x < 0.04%
Figure 7.3 (d)	1.0% < x < 1.2%
Figure 7.3 (e)	0.01% < x < 0.04%
Figure 7.3 (f)	0.01% < x < 0.04%
Figure 7.4	0.002% < x < 0.003%
Figure 7.5 (a)	0.01% < x < 0.05%
Figure 7.5 (b)	0.01% < x < 0.05%
Figure 7.5 (c)	0.01% < x < 0.05%
Figure 7.5 (d)	0.6% < x < 1.0%
Figure 7.5 (e)	0.6% < x < 1.0%
Figure 7.5 (f)	0.6% < x < 1.0%
Figure 7.6 (a)	1.9% < x < 2.6%
Figure 7.6 (b)	2.0% < x < 2.7%
Figure 7.6 (c)	2.0% < x < 2.7%
Figure 7.6 (d)	2.5% < x < 3.1%
Figure 7.6 (e)	1.9% < x < 2.6%
Figure 7.6 (f)	1.9% < x < 2.6%
Figure 7.7	0.002% < x < 0.003%
Figure 7.8 (a)	0.01% < x < 0.05%
Figure 7.8 (b)	2.5% < x < 3.1%
Figure 7.8 (c)	2.2% < x < 2.9%
Figure 7.8 (d)	2.2% < x < 2.9%

Table 10.1: % Confidence Intervals

Figure	Percentile Confidence Variation (x) over Mean Value
Figure 7.8 (e)	2.5% < x < 3.1%
Figure 7.8 (f)	0.01% < x < 0.05%
Figure 7.9 (a)	0.01% < x < 0.05%
Figure 7.9 (b)	0.01% < x < 0.05%
Figure 7.9 (c)	0.01% < x < 0.05%
Figure 7.9 (d)	1.0% < x < 1.4%
Figure 7.9 (e)	0.01% < x < 0.05%
Figure 7.9 (f)	0.01% < x < 0.05%
Figure 7.10	0.002% < x < 0.003%
Figure 7.11 (a)	0.01% < x < 0.05%
Figure 7.11 (b)	0.01% < x < 0.05%
Figure 7.11 (c)	0.01% < x < 0.05%
Figure 7.11 (d)	1.0% < x < 1.4%
Figure 7.11 (e)	0.01% < x < 0.05%
Figure 7.11 (f)	0.01% < x < 0.05%
Figure 7.12	0.002% < x < 0.003%
Figure 7.13	0.01% < x < 0.04%
Figure 7.14 (a)	0.01% < x < 0.05%
Figure 7.14 (b)	0.01% < x < 0.05%
Figure 7.15 (a)	0.01% < x < 0.05%
Figure 7.15 (b)	0.02% < x < 0.05%
Figure 7.16 (a)	5.5% < x < 5.8%
Figure 7.16 (b)	5.5% < x < 5.8%
Figure 7.17 (a)	0.01% < x < 0.05%
Figure 7.17 (b)	0.02% < x < 0.05%
Figure 7.18 (a)	0.002% < x < 0.003%
Figure 7.18 (b)	0.002% < x < 0.003%
Figure 7.19 (a)	0.002% < x < 0.003%
Figure 7.19 (b)	0.002% < x < 0.003%
Figure 7.20 (a)	0.002% < x < 0.003%
Figure 7.20 (b)	0.002% < x < 0.003%
Figure 7.21 (a)	0.01% < x < 0.05%
Figure 7.21 (b)	0.01% < x < 0.05%
Figure 7.21 (c)	0.01% < x < 0.05%
Figure 7.21 (d)	1.0% < x < 1.4%
Figure 7.21 (e)	0.01% < x < 0.05%
Figure 7.21 (f)	0.01% < x < 0.05%
Figure 7.22 (a)	0.004% < x < 0.005%
Figure 7.22 (b)	0.004% < x < 0.005%
Figure 7.22 (c)	0.004% < x < 0.005%

Table 10.2: % Confidence Intervals (cont.)

References

[1] Requirements for the UMTS terrestrial radio access system (UTRA), Technical Report 21.01U, 3GPP. 1997.

[2] Feasibility study for enhanced uplink for UTRA FDD, Technical Report 25.896. *3GPP*, 2004.

[3] Matlab, version 7.0.1.24704 service pack 1. *The MathWorks Inc*, 2004.

[4] 3GPP website http://www.3gpp.org, October 2005.

[5] http://www.umts-forum.org/servlet/dycon/ztumts/umts/Live/en/umts/resources_fastfacts. October 2005.

[6] 3GPP. Technical Specification Group Radio Access Network; Physical layer procedures (FDD) (Release 1999). March 2002.

[7] E. Altman. Capacity of multi-service cellular networks with transmission-rate control: A queueing analysis. *ACM Mobicom'02*, pages 23–28, September 2002.

[8] E. Altman. Rate control and qos-related capacity in wireless communications. *Keynote Speech at Quality of Future Internet Services, QoFIS*, October 2003.

[9] Eitan Altman. Capacity of Multi-service Cellular Networks with Transmission-Rate Contro: A Queueing Analysis. *Mobicom*, September 2002.

[10] Alex Brand and Hamid Aghvami. Multiple Access Protocols for Mobile Communications GPRS, UMTS and Beyond. *John Wiley & Sons, Ltd*, 2002.

[11] EIA/TIA InterimStandard-95. Mobile station-base station compatibility standard for dualmode wideband spread spectrum cellular system. 1993.

[12] Ericsson. Basic concepts of WCDMA radio access network. 2001.

[13] Ericsson. WCDMA evolved, the first step - HSDPA. *in the Proc. of IFIP Networking 2005*, May 2004.

[14] Gabor Fodor. On Multi-Cell Admission Control in CDMA Networks. September 2005. under submission.

[15] Gabor Fodor and M. Telek. Performance Analysis of the Uplink of a CDMA Cell Supporting Elastic Services. *in the Proc. of IFIP Networking 2005*, pages 205–216, 2005.

[16] Shkumbin Hamiti, Eero Nikula, Janne Parantainen, Timo Rantalainen, Benoist Sbire, and Guillaume Sbire. GSM/EDGE Radio Access Network (GERAN) - Evolution of GSM / EDGE towards 3G Mobile Services. *Nokia Research Center*, 2001.

[17] M. Hata. Empirical formula for propagation loss in land mobile radio services. *IEEE Trans. Veh. Tech.*, 29(3):317–325, 1980.

[18] H. Holma and A. Toskata. WCDMA for UMTS, Third Edition, J. Wiley & Sons. 2003.

[19] Telecompetition Inc. 3G Wireless Data Traffic Characteristics - Commercial Report. June 2001.

[20] Jaana Laiho, Achim Wacker, and Tomas Novosad. Radio Network Planning and Optimisation for UMTS. *John Wiley & Sons, Ltd*, page 189, 2002.

[21] Jose Carnero Outes, Alborg University. *Uplink Capacity Enhancement in WCDMA, Synchronised Schemes and Fast Packet Scheduling.* PhD thesis, March 2004.

[22] I. Koo, J. Ahn, H. A. Lee, and K. Kim. Analysis of Erlang capacity for the multimedia DS-CDMA systems. *IEICE Trans. Fundamentals*, May 1999.

[23] Matias Nironen. Admission Control in HSDPA/HSUPA. *Tampere University of Technology - Department of Information Technology*, 2005.

[24] J. W. Roberts. Multi-service traffic performance in mobile networks. *France Telecom Recherche and Developpment*, January 2003.

[25] N. Wiberg. Casper 1.0. February 2000.